

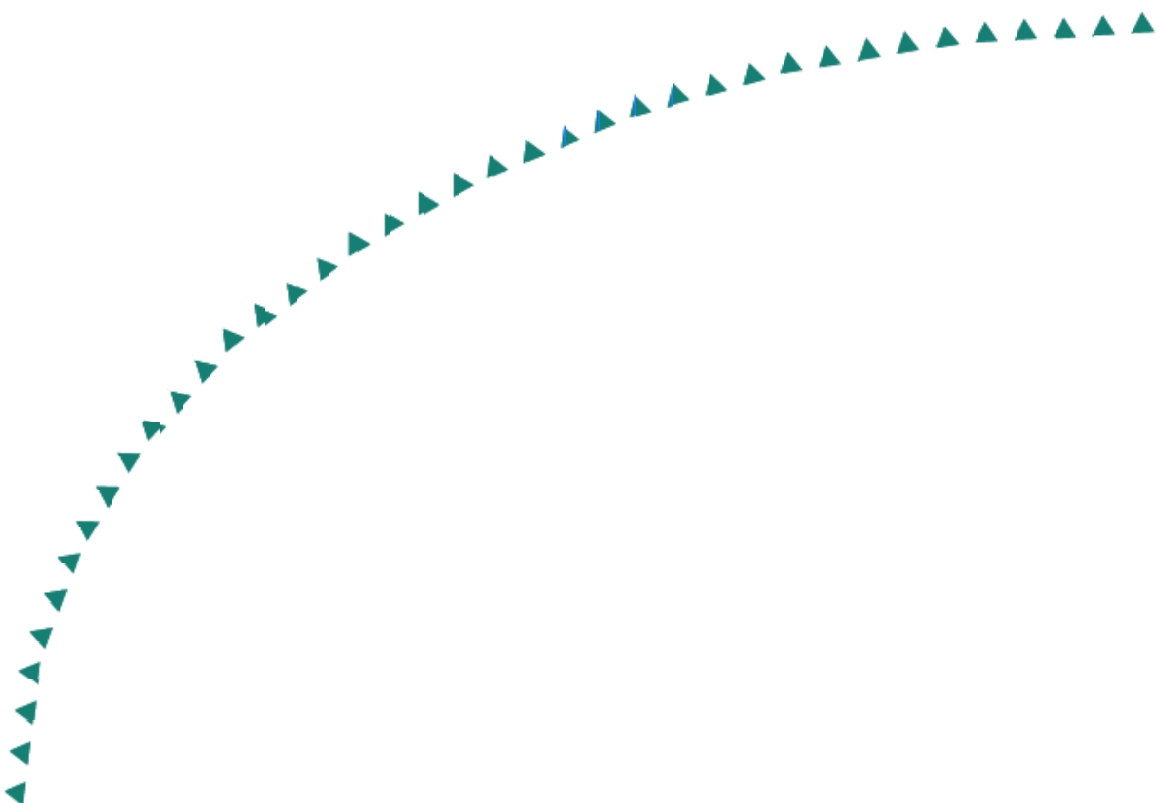
2003-18

Final Report

**Fatigue Evaluation of Steel
Box-Girder Pier Caps: Bridge 69832**



Research



Technical Report Documentation Page

1. Report No. MN/RC – 2003-18	2.	3. Recipients Accession No.	
4. Title and Subtitle FATIGUE EVALUATION OF STEEL BOX-GIRDER PIER CAPS: BRIDGE 69832		5. Report Date March 2004	
		6.	
7. Author(s) Clifford J. Youngberg, Robert J. Dexter, and Paul M. Bergson		8. Performing Organization Report No.	
9. Performing Organization Name and Address University of Minnesota Department of Civil Engineering 122 CivE, 500 Pillsbury Dr. S.E. Minneapolis, MN 55455-0116		10. Project/Task/Work Unit No.	
		11. Contract (C) or Grant (G) No. (c) 81655 (wo) 13	
12. Sponsoring Organization Name and Address Minnesota Department of Transportation Office of Research Services 395 John Ireland Boulevard Mail Stop 330 St. Paul, Minnesota 55155		13. Type of Report and Period Covered Final Report	
		14. Sponsoring Agency Code	
15. Supplementary Notes http://www.lrrb.gen.mn.us/PDF/200318.pdf			
16. Abstract (Limit: 200 words) Steel pier caps designed such that the longitudinal girders are continuous through the pier cap are subject to significant torsion due to differences in the girder end moments and may be susceptible to fatigue cracking. One such pier cap, part of Bridge 69832 on northbound Interstate 35 heading into the business district of Duluth, was instrumented, load tested, and modeled. Several similar pier caps had developed fatigue cracking at different details. The cracks are due to high stress ranges that occur in the corners of the box section. None of these cracks are presently a threat to the structural integrity of the pier caps. Most of the cracks are limited to the welds and will eventually arrest as they grow larger with minimal structural consequences. Therefore the recommendation for these cracks is to inspect them carefully every two years and not repair them. However, holes must be drilled at least at one location where the cracks are presently in the web plates of the pier caps. Recommendations are presented for inspection of similar integral pier caps and for design of new steel pier caps.			
17. Document Analysis/Descriptors Steel Pier Cap Distortion Induced Fatigue Fracture Critical		18. Availability Statement No restrictions. Document available from: National Technical Information Services, Springfield, Virginia 22161	
19. Security Class (this report) Unclassified	20. Security Class (this page) Unclassified	21. No. of Pages 67	22. Price

Fatigue Evaluation of Steel Box-Girder Pier Caps: Bridge 69832

Clifford J. Youngberg
Robert J. Dexter
Paul M. Bergson

Department of Civil Engineering
University of Minnesota
500 Pillsbury Drive SE
Minneapolis, MN 55455-0116

March 2004

Published by:

Minnesota Department of Transportation
Research Services
Mail Stop 330
395 John Ireland Boulevard
Saint Paul, MN 55155-1899

This report represents the results of research conducted by the author and does not necessarily represent the view or policy of the Minnesota Department of Transportation and/or the Center for Transportation Studies. This report does not contain a standard or specified technique.

ACKNOWLEDGEMENTS

Funding for this research was provided by the Minnesota Department of Transportation (Mn/DOT). We would like to thank the many people from Mn/DOT who have helped with this research including Dan Dorgan, Gary Peterson, Erik Wolhowe, Pete Wilson, Dow Rychalk, Brad Johnson, Dave Davidson, and the Duluth maintenance crews. The review and assistance of the Office of Research Services is also appreciated.

We would also like to thank all the people from the University of Minnesota that helped in this project, especially Eric Corwin, Yuying Hu, Jessica Mitchell, Angela Kingsley, and Jon Wacker for their help with instrumentation and the truck tests. I also thank Eric Corwin for his help with the finite element modeling and analysis. Supercomputing resources were provided by the Minnesota Supercomputing Institute.

METRIC CONVERSION FACTORS

Approximate Conversions to Metric Measures

Symbol	When You Know	Multiply By	To Find	Symbol
LENGTH				
in	inches	* 2.5	centimeters	cm
ft	feet	30	centimeters	cm
yd	yards	0.9	meters	m
mi	miles	1.6	kilometers	km
AREA				
in ²	square inches	6.5	square centimeters	cm ²
ft ²	square feet	0.09	square meters	m ²
yd ²	square yards	0.8	square meters	m ²
mi ²	square miles	2.6	square kilometers	km ²
	acres	0.4	hectares	ha
MASS (WEIGHT)				
oz	ounces	28	grams	g
lb	pounds	0.45	kilograms	kg
	short tons (2000 lb)	0.9	tonnes	t
VOLUME				
tsp	teaspoons	5	milliliters	ml
tbsp	tablespoons	15	milliliters	ml
fl oz	fluid ounces	30	milliliters	ml
c	cups	0.24	liters	l
pt	pints	0.47	liters	l
qt	quarts	0.95	liters	l
gal	gallons	3.8	liters	l
ft ³	cubic feet	0.03	cubic meters	m ³
yd ³	cubic yards	0.76	cubic meters	m ³
TEMPERATURE (EXACT)				
°F	Fahrenheit temperature	5/9 (after subtracting 32)	Celsius temperature	°C

* 1 in = 2.54 (exactly).

Approximate Conversions from Metric Measures

Symbol	When You Know	Multiply By	To Find	Symbol
LENGTH				
mm	millimeters	0.04	inches	in
cm	centimeters	0.4	inches	in
m	meters	3.3	feet	ft
m	meters	1.1	yards	yd
km	kilometers	0.6	miles	mi
AREA				
cm ²	square centimeters	0.16	square inches	in ²
m ²	square meters	1.2	square yards	yd ²
km ²	square kilometers	0.4	square miles	mi ²
ha	hectares (10,000 m ²)	2.5	acres	
MASS (WEIGHT)				
g	grams	0.035	ounces	oz
kg	kilograms	2.2	pounds	lb
t	tonnes (1000 kg)	1.1	short tons	
VOLUME				
ml	milliliters	0.03	fluid ounces	fl oz
l	liters	0.125	cups	c
l	liters	2.1	pints	pt
l	liters	1.06	quarts	qt
l	liters	0.26	gallons	gal
m ³	cubic meters	35	cubic feet	ft ³
m ³	cubic meters	1.3	cubic yards	yd ³
TEMPERATURE (EXACT)				
°C	Celsius temperature	9/5 (then add 32)	Fahrenheit temperature	°F

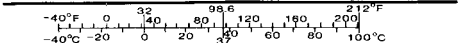


TABLE OF CONTENTS

Chapter 1 – Introduction	1
1.1 Problem Statement	1
1.2 Objective	1
1.3 Scope of Report	2
Chapter 2 – Description of Bridge 69832	3
2.1 Description	3
2.2 Fatigue Cracks	6
2.3 Fatigue Background	10
2.4 Detail Inspection	12
2.5 Mechanism for Failures	15
Chapter 3 – Field Instrumentation and Testing	17
3.1 Instrumentation Plan	17
3.1.1 Phase 1	17
3.1.2 Phase 2	22
3.2 Test Descriptions and Data Retrieval	24
3.2.1 Mn/DOT Truck Test Descriptions	24
3.2.2 Live Traffic Monitoring	27
3.2.3 Data Collection	28
Chapter 4 – Data Analysis from Field Instrumentation	29
4.1 Truck Test Results	29
4.1.1 Test 1	29
4.1.2 Test 2	31
4.1.3 Test 3	33
4.1.4 Test 4	34
4.1.5 Additional Testing	34
4.2 Live Traffic Analysis	37
Chapter 5 – Finite Element Modeling and Analysis	43
5.1 Three-dimensional Grillage Model	43
5.2 Shell Element Models	49
5.2.1 Pier Cap 5 – Uncracked	50
5.2.2 Pier Cap 5 – Cracked	50
5.2.3 Pier Cap 5 – Retrofit	50
5.2.4 Comparison and Analysis	50
Chapter 6 – Summary and Recommendations	55
6.1 Crack Type 1	55
6.2 Crack Type 2	57
6.3 Crack Type 3	58
References	59

LIST OF FIGURES

Figure 2.1:	Bridge 69832	3
Figure 2.2:	Drawing of plan view of Bridge 69832	4
Figure 2.3:	Steel pier cap with girders bearing on top	4
Figure 2.4:	Steel pier cap with girders continuous through pier cap	5
Figure 2.5:	Dimensions of typical cross section	5
Figure 2.6:	Cross-section of Pier Cap 5 showing crack type 1	6
Figure 2.7:	Crack type 1	7
Figure 2.8:	Cross-section of Pier Cap 9 showing crack type 2	8
Figure 2.9:	Crack type 2	8
Figure 2.10:	Cross-section of Pier Cap 11 showing crack type 3	9
Figure 2.11:	Crack type 3	9
Figure 2.12:	S-N curves	11
Figure 2.13:	Location of weld measurements	12
Figure 2.14:	Crack-like notch between fillet welds in a cruciform connection	14
Figure 2.15:	Exaggerated displaced shape showing concentration of distortion in lower cell	16
Figure 3.1:	Welding of a strain gage	18
Figure 3.2:	Girder A gage placement	19
Figure 3.3:	Pier cap gage placement	20
Figure 3.4:	Bracket design plans	21
Figure 3.5:	Installation of bracket	22
Figure 3.6:	Interior of Pier Cap 5 gage placement Girder D	23
Figure 3.7:	Interior of Pier Cap 5 LVDT placement	24
Figure 3.8:	Mn/DOT three-axle truck	25
Figure 3.9:	Truck Test 1	26
Figure 3.10:	Truck Test 2	26
Figure 3.11:	Truck Test 3	27
Figure 3.12:	Truck Test 4	27
Figure 3.13:	PC9000 data acquisition system	28
Figure 4.1:	Strain gage readings from midspan locations during Test 1	30
Figure 4.2:	Composite action from midspan of Girder C	31
Figure 4.3:	Horizontal LVDT readings showing differential movement of girders (Test 1)	31
Figure 4.4:	Load distribution among the girders during Test 2	32
Figure 4.5:	Horizontal LVDT readings showing differential movement of girders (Test 2)	33
Figure 4.6:	Strain gage readings from midspan locations during Test 3	34
Figure 4.7:	Horizontal LVDT readings showing differential movement of girders (Test 3)	34
Figure 4.8:	Inclinometer readings from Mn/DOT Snooper	35
Figure 4.9:	Linear interpolation of horizontal LVDT data for a vehicle in right lane	36
Figure 4.10:	Linear interpolation of midspan strain gage data for a vehicle in right lane	37

Figure 4.11:	Stiffener Strains from interior of pier cap	38
Figure 4.12:	Shearing of the top and bottom cells	39
Figure 4.13:	Stress range distribution for gage S-GC-F-3 (W)	41
Figure 5.1:	Three-dimensional grillage model	43
Figure 5.2:	Stress comparison on bottom flange of girders at midspan for loading in the right lane	46
Figure 5.3:	Stress comparison on bottom flange of girders at midspan for loading in the left lane	46
Figure 5.4:	Through depth stresses on Girder C at midspan due to 50-kip truck	47
Figure 5.5:	Stress history as load moves across the bridge	48
Figure 5.6:	Shell element model integrated into grillage model	49
Figure 5.7:	Stiffener stresses for the three shell element models	51
Figure 5.8:	Stress distribution at Girder D for the three shell element Models	52
Figure 5.9:	Intermediate stiffener detail	52
Figure 5.10:	Maximum stresses in intermediate stiffeners due to 50-kip truck in right lane	53
Figure 5.11:	Stress distribution in intermediate Stiffener C-D	53
Figure 6.1:	Retrofit for intersection of girder and pier cap	56
Figure 6.2:	Hole drilling retrofit	57

LIST OF TABLES

Table 2.1:	Table with detail constants	11
Table 2.2:	Summary of detail inspection	13
Table 3.1:	Mn/DOT truck weights and dimensions	24
Table 4.1:	Truck Test results summary	36
Table 4.2:	Readings for a typical 50-kip truck	40
Table 4.3:	Number of events exceeding each stress level for gage S-GC-F-3 (W)	41
Table 5.1:	Applied load calculations for 50-kip truck	44

LIST OF EQUATIONS

Equation 2.1:	Equation for nominal fatigue resistance (AASHTO)	10
Equation 2.2:	Reduction factor of plates loaded in tension	13
Equation 4.1:	Miner's Rule	42

EXECUTIVE SUMMARY

Bridge 69832, which carries northbound Interstate 35 into Duluth, has had multiple fatigue cracks on the fracture-critical steel pier caps where the girders are integral with the pier caps. Instrumentation was installed around Pier Cap 5 to determine the response of the bridge under loading. Multiple truck tests were conducted using Mn/DOT three-axle trucks to provide known loads for calibration. Data were collected from the truck tests and from live traffic to determine the frequency and magnitude of the loads Bridge 69832 carries.

Finite element models were created of the 4-span section around Pier Cap 5. Grillage models composed of frame elements only were created for comparing the models to the data collected from the field instrumentation. A shell element model of Pier Cap 5 was then created within the grillage model to perform more detailed analysis of the areas with the fatigue cracking problems.

The data collected from the field and the results from the finite element models confirmed that the cracks are due to torsion of the pier caps due to different girder end moments under traffic loading. As the rectangular cross section distorts, high stress ranges occur at the corners. The location of the high stress ranges is dependent on the detail inside the pier cap.

None of these cracks are presently a threat to the structural integrity of the pier caps. Most of the cracks are limited to the welds and will eventually arrest as they grow larger with minimal structural consequences. Therefore the recommendation for these cracks is to inspect them carefully every two years and not repair them. However, on the north side at Girder D of Pier Cap 9, the cracks are presently in the web plates of the pier caps and these must be repaired as soon as possible.

For further inspections of Bridge 69832 and bridges with similar integral pier caps, close attention should be paid to details that have stiffeners that are milled to bear at the tension flange instead of being attached. These details are susceptible to out of plane distortion. Also details that divide the pier cap into two cells where one cell is more flexible than the other should be inspected more carefully. Larger deformation will concentrate in these more flexible cells and fatigue problems can occur at the corners. Poor fit up of the pieces may lead to gaps and associated inadequate weld throat. Welds with multiple passes, excess slag, gas pockets, and any other defects should be noted.

Similar pier caps with integral girders should be examined to estimate the distribution of the moments among the girders. If there is a large difference between the end moments of adjacent girders, there is a potential for these types of cracks. The next step would be to look at the detail and determine where the stress due to the torsion will concentrate.

CHAPTER 1: INTRODUCTION

1.1 Problem Statement

Steel pier caps are usually box sections and are usually only used when there is a large span between piers, often to span over roadways and/or railways under the bridge. If there is adequate clearance, the longitudinal girders bear on the top of the steel pier caps that are therefore subject primarily to flexure – there are few problems with this type of pier cap. However, when clearance is limited, the longitudinal girders may be designed to be continuous through the pier cap, subjecting the pier caps to significant torsion due to differences in the girder end moments as well as flexure. This type of pier cap may be susceptible to fatigue cracking.

Bridge 69832 on northbound Interstate 35 heading into the business district of Duluth features both types of steel pier caps. This bridge spans multiple railroad lines (some of which are now abandoned) and is subjected to heavy truck traffic. Because of the railroad lines, pier spacing varies with several of the piers located away from the bridge superstructure. Concrete pier caps are used when the piers are located below the bridge superstructure and steel pier caps are used when one of the piers is located away from the bridge superstructure. Some of the steel pier caps were designed with the girders bearing on top of the pier caps, while others were designed with the girders continuous through the pier caps. Fatigue cracking has occurred at multiple locations in the latter type of pier cap. The location of the cracks is dependent on the specific details used for the pier cap. Steel pier caps are fracture-critical members and therefore the behavior of these steel pier caps, the causes of the fatigue cracks, and the effects of several repair schemes were evaluated in detail.

1.2 Objectives and Approach

The main objectives of this project were to determine the cause and significance of the fatigue cracks in the steel pier caps of Bridge 69832 and to design and assess the effectiveness of several alternative repair schemes. Broader secondary objectives include understanding the general behavior of steel pier caps with integral continuous girders, identifying characteristics of steel pier caps that make them susceptible to fatigue to focus inspection of existing structures, and recommending better details for future designs.

To achieve these objectives, instrumentation was installed on one of the pier caps and the adjacent girders to characterize the overall bridge response, pier cap deformations, and localized stress ranges under controlled loading as well as open traffic. Finite element models were then created and calibrated with regard to the measured data to better understand the behavior of the bridge and to simulate repair and retrofit options. These data were analyzed to determine the causes of the fatigue cracking. The most suitable repair schemes were further developed and recommended.

1.3 Scope of Report

This report begins with a description of Bridge 69832 and its function in chapter 2. This chapter also includes a description of the fatigue cracking that is taking place, a review of fatigue design practice, a detailed inspection, and lastly the mechanism behind the high stress ranges. In chapter 3, the location and installation of instrumentation is described. Also included are descriptions of the truck tests that were performed. Analysis of measurements taken during the truck tests and from live traffic is covered in chapter 4. Descriptions and the analysis of all finite element models comprise chapter 5. Lastly, in chapter 6, proposed recommendations and retrofits for addressing the fatigue problems are covered.

CHAPTER 2: DESCRIPTION OF BRIDGE 69832

2.1 Description of Bridge

Bridge 69832, constructed in 1967, is shown in Figure 2.1. It carries two lanes of northbound Interstate 35 into downtown Duluth and the port area. Because it is the main artery into downtown Duluth and the port area, the bridge is subjected to heavy truck traffic.



Figure 2.1: Bridge 69832

As shown in the plan in Figure 2.2, Bridge 69832 is a 12-span, 4 girder bridge that crosses multiple rail lines. The piers are numbered 1 through 11 beginning at the south end of the bridge. The girders are labeled A through D going from west to east. Concrete pier caps were used when the pier columns are located directly below the bridge superstructure and steel pier caps are used when one or both of the pier columns is located away from the bridge superstructure.

Of the steel-box designs, the first type had the girders resting on sole plates attached to the top of the steel-box pier cap (Figure 2.3). These have shown no problems with fatigue, as the girders are free to move separately from the pier cap.

The second type of steel-box pier cap was designed so that the girders are continuous through the pier cap (Figure 2.4). It is assumed these pier caps were designed with the girders integral to the pier cap to meet clearance requirements for crossing railroad lines. The pier caps are deeper than the girders, so the box consists of two cells at those cross sections where the girders pass through. The depth at which the girders pass through the pier caps varied affecting the stiffener details. Figure 2.5 gives the dimensions for a typical cross section of this type of pier cap.

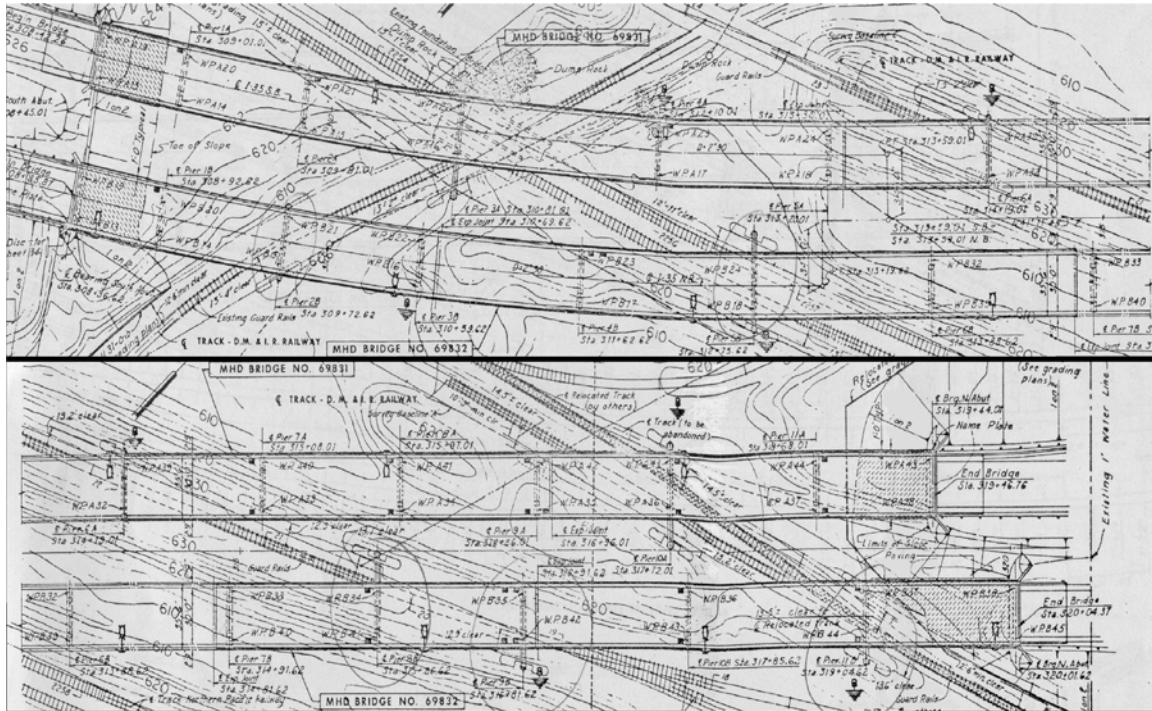


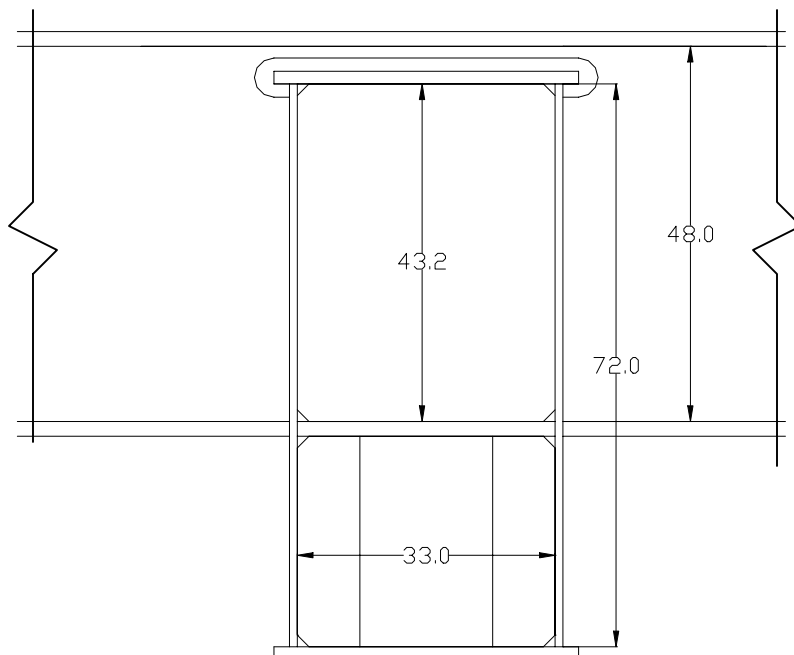
Figure 2.2: Drawing of plan view of Bridge 69832



Figure 2.3: Steel pier cap with girders bearing on top



Figure 2.4: Steel pier cap with girders continuous through pier cap



Figures 2.5: Dimensions of typical cross section

In the integral-type pier cap, the girders are restrained by the torsional stiffness of the pier cap, resulting in applied torque to the pier cap due to differences in end moments among the four girders. The twisting of the pier cap due to passing of trucks results in shear distortion of the cross section and associated high tensile stress ranges in the corners. Because of these unanticipated stress ranges, fatigue cracking has been observed at various details in these pier caps. Since steel pier caps are fracture critical, the fatigue cracks are of even greater concern.

2.2 Fatigue Cracks in Bridge 69832

Three different crack types have been observed on Bridge 69832, depending on the stiffener details of the pier cap. These cracks were first documented in June of 1999 (1). Crack type 1 occurred at the weld connecting the stiffener to the bottom flange continuity plate inside the pier cap (Figure 2.6). Cracks like this have occurred at Girders A, B, and C on Pier Cap 5. All of these cracks are located on the stiffeners on the North side only. As shown in Figure 2.7, these cracks propagate through the welds but have not propagated into the base metal. Eventually, the cracks may completely sever the weld of the stiffener to the continuity plate, which so far has only occurred at Girder C (2). Once this occurs, however, the crack is isolated since there isn't any path for the crack to propagate further. Therefore the consequences of crack type 1 are limited.

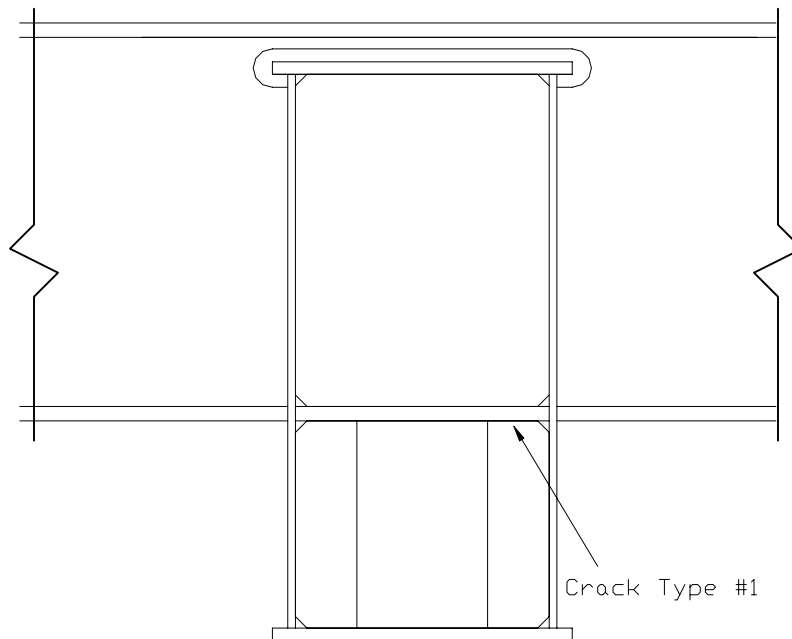


Figure 2.6: Cross-section of Pier Cap 5 showing crack type 1

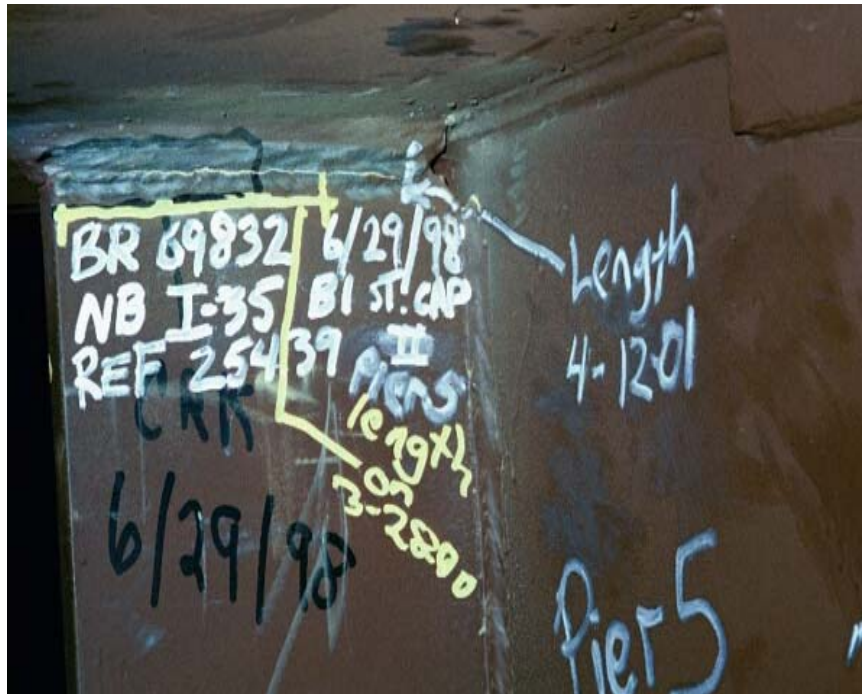


Figure 2.7: Crack type 1

Crack type 2 occurred at the termination of the vertical weld connecting the bulkhead to the pier cap web (Figure 2.8). It was customary at the time this bridge was designed to not weld stiffeners to the tension flange, so this bulkhead was not welded to the bottom flange of the pier cap. (This practice has subsequently been identified as contributing to distortion-induced fatigue, and there have been requirements in the AASHTO specifications since 1985 to require a positive connection of such a stiffener as this bulkhead to all elements of the cross section.) Crack type 2 has occurred at girder D of pier cap 9 and Girders A and D of Pier Cap 11. The cracks on the north side in Girder D of Pier Cap 9 have propagated into the web of the pier cap (Figure 2.9), which is potentially a very serious condition (2). All others currently are propagating up the weld, which should limit the consequences to separation of the bulkhead from the web.

Crack type 3 is a crack located at the toe of the weld connecting the girder web to the exterior of the pier cap web (Figure 2.10). It has only been found on Girder C of pier cap 11 on the north side, and is not propagating into the base metal (Figure 2.11)(2). It is believed that this crack is driven by the bending stresses in the web, which will decrease as the crack extends eventually arresting the crack. Therefore, it is believed that the consequences of this crack are limited, provided sufficient shear capacity of the web welds remain after the crack arrests.

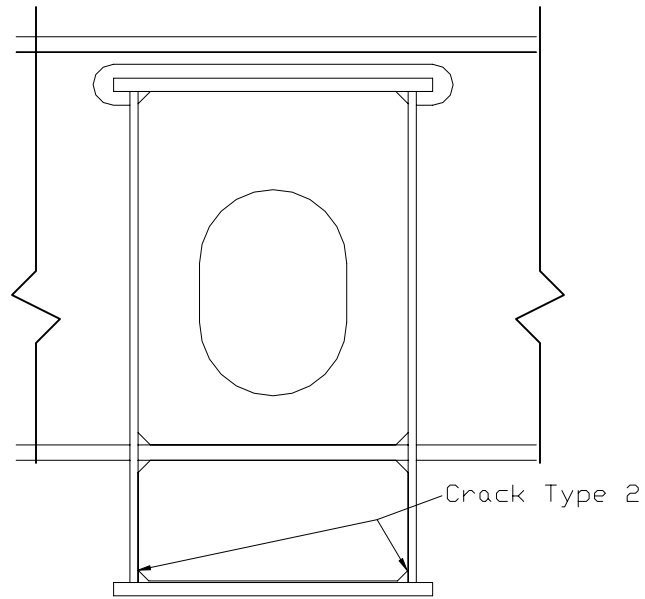


Figure 2.8: Cross-section of pier cap 9 showing crack type 2



Figure 2.9: Crack type 2

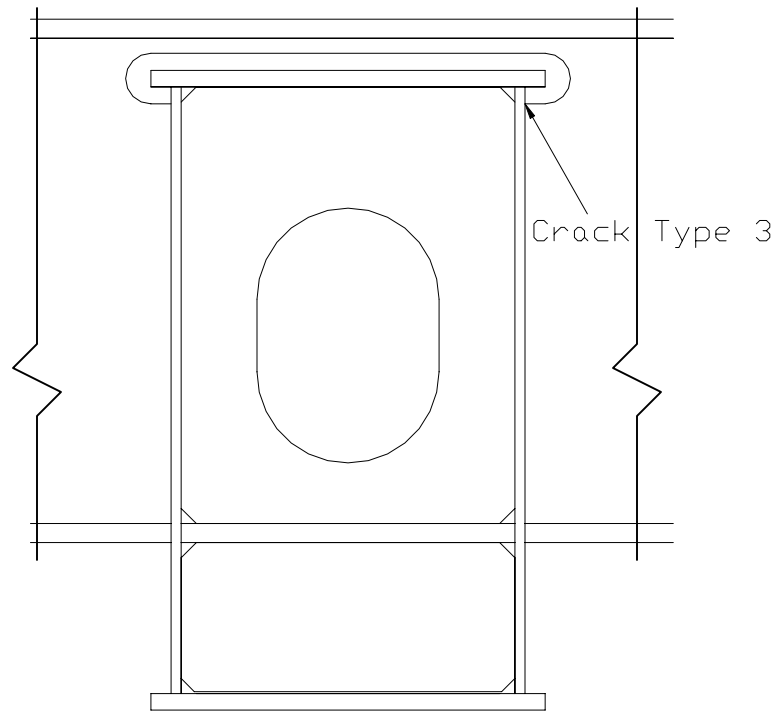


Figure 2.10: Cross-section of pier cap 11 showing crack type 3

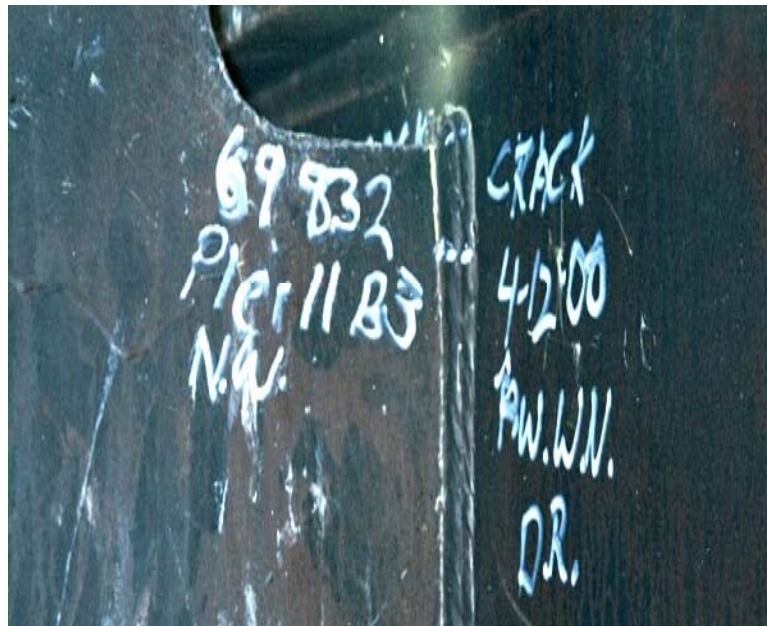


Figure 2.11: Crack type 3

2.3 Fatigue Background

This section gives an overview of design and evaluation procedures for fatigue. The American Association of State Highway and Transportation Officials (AASHTO) LRFD Bridge Design Specification provisions on fatigue will be reviewed, although there is little difference among other steel design specifications.

Present fatigue design specifications were adopted in the mid-1970s, therefore some of the bridges built before this time may be susceptible to fatigue cracking (3). These problems are, for the most part, relatively minor and usually can be corrected with inexpensive retrofits (3). Steel bridges that have been built in the last few decades have not and should not have any significant problems with fatigue and fracture (4). The plans for Bridge 69832 were completed in 1965; therefore the fatigue cracks are not entirely unexpected.

The fatigue life of a detail is dependent upon the stress range and the number of cycles applied. For design purposes, most details for steel structures have been classified into 8 categories, called detail categories, based on their fatigue resistance (5). These categories are labeled A, B, B', C, C', D, E, and E' with Category A having the highest resistance to fatigue and Category E' having the lowest. The fatigue resistance of each category is represented by a lower-bound S-N curve that is derived from fatigue test data and represents 97.5 percent survival, as shown in Figure 2.12. The following Equation 2.1 for the allowable stress range due to the fatigue truck loading $(\Delta F)_N$ represents the S-N curves (5):

$$(\Delta F)_N = \left(\frac{A}{N} \right)^{1/3} \geq \frac{(\Delta F)_{th}}{2}$$

for which:

A = constant specific to detail category (ksi^3)

$(\Delta F)_{th}$ = constant-amplitude fatigue limit – CAFL (ksi)

and N = $(365)(75)n(ADTT)_{SL}$

where:

n = number of stress range cycles per truck passage

$(ADTT)_{SL}$ = average daily truck traffic for single lane

Equation 2.1: Equation for nominal fatigue resistance (AASHTO)

The constants A and $(\Delta F)_{th}$ are summarized in Table 2.1. The fatigue truck in the AASHTO LRFD Specifications is 0.75 times the HS-20 design truck, or a gross-vehicle weight of 54 kips, representing the effective load of a variable series of trucks. The constant-amplitude fatigue limit (CAFL), designated $(\Delta F)_{th}$ in AASHTO, is the stress range below which fatigue cracking does not occur. Equation 2.1 indicates that the allowable stress range need not be taken less than half the CAFL. In effect, this indicates that the fatigue life is unlimited if the stress range from a load approximately twice the load of the fatigue truck is less than the CAFL.

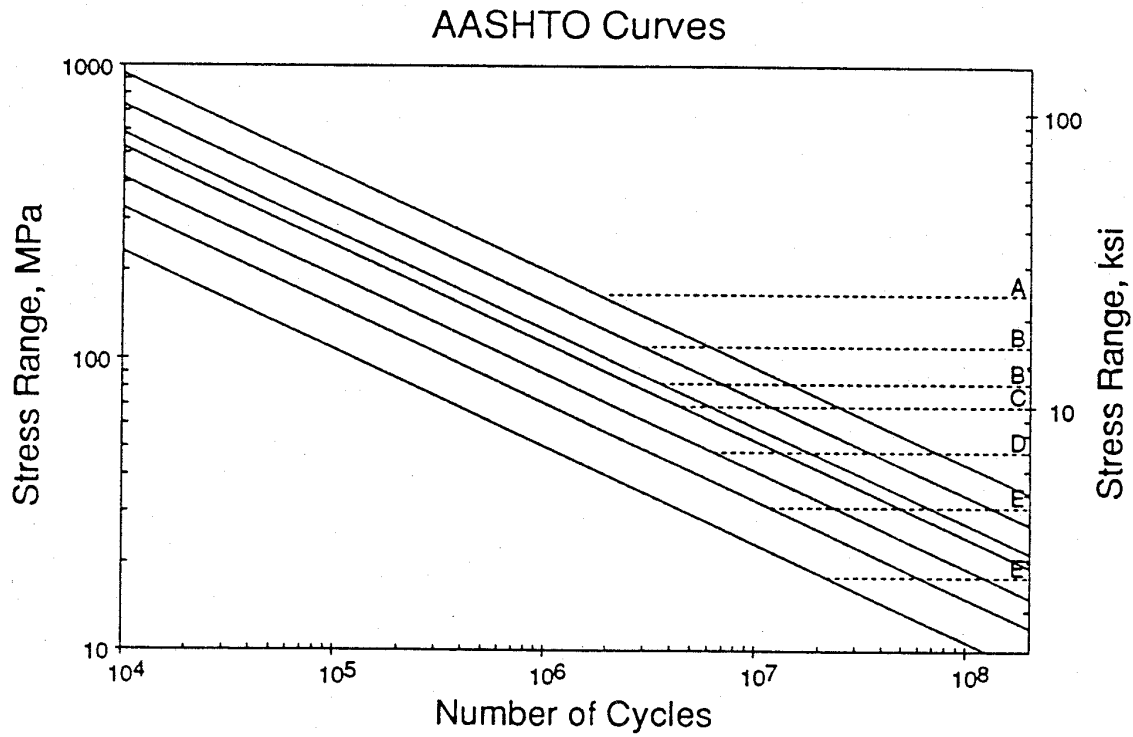


Figure 2.12: AASHTO S-N curves

Table 2.1: AASHTO detail constants

Detail Category	Detail Constant A (ksi ³)	(ΔF) _{th} (ksi)
A	2.5E+10	24
B	1.2E+10	16
B'	6.2E+09	12
C	4.4E+09	10
C'	4.4E+09	12
D	2.2E+09	7
E	1.1E+09	4.5
E'	4.0E+08	2.6

In Bridge 69832, the details where fatigue cracking has occurred are Category C. The Category C detail has a (ΔF)_{th} of 10 ksi, therefore if the stress range exceeds 10 ksi on a daily basis or more frequently, the detail has a finite life and cracking will occur at some point.

2.4 Detailed Inspection

On Pier Cap 5 an inspection of various details was performed to determine any discrepancies between those detailed and those constructed. Measurements were taken of the weld sizes, the heights and widths, and the size of gaps at various locations. This inspection was performed to see if there was an explanation for why details on only one side of the box cracked in some cases. The location of where the measurements were taken is shown in Figure 2.13 and a summary of the results compared to the drawing requirements is given in Table 2.2.

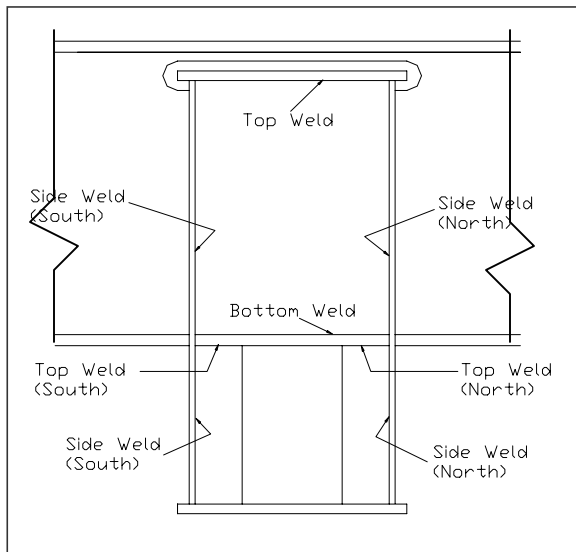


Figure 2.13: Location of weld measurements

Measuring the height of the lower cell on either side showed up to a $\frac{1}{4}$ " difference from the north to the south. This indicates that there is a slight inclination in the girder as it passes through the pier cap. It was also noticed that gaps were present at the bottom of the stiffeners, where in the plans they are indicated to be milled to bear.

The largest discrepancy was found in the size of fillet weld connecting the stiffener to the bottom flange continuity plate. The plans call for a $\frac{3}{8}$ " weld while those measured were greater than $\frac{3}{4}$ ". It appeared that the stiffener was not flush against the continuity plate and that the larger weld may have been required to cover this gap. This would decrease the throat thickness of the weld and thus the strength and fatigue resistance of the weld.

When pairs of transverse fillet welds are used to attach a plate loaded in tension a reduction factor (R_F) calculated as in Equation 2.2 is applied to the design stress range for fatigue (6). This reduction factor accounts for the possibility of fatigue cracking through the throat of the weld. The unfused space between the fillet welds acts as a preexisting crack at the root of the weld. The reduction factor governs on thick plates as the length of the preexisting crack is increased. .

Table 2.2: Summary of detail inspection

	Detailed	Girder A	Girder B	Girder C	Girder D
Top Cell					
Height		43.125	42	42.125	43.125
Width	33"	32.75	32.625	32.75	33.25
Top Weld	3/8"	(1/4)	3/8 (3/8)	3/8 (3/8)	1/2 (1/2)
Bottom Weld	3/8"	(1/2)	1/2 (5/8)	3/8 (1/2)	1/2 (1/2)
Side Weld (South)	3/16"	(1/4)	1/4 (1/4)	1/4 (3/16)	3/8 (1/4)
Side Weld (North)	3/16"	(5/16)	1/4 (1/4)	3/16 (3/16)	1/4 (1/4)
Bottom Cell					
Height (South)		26.6875	27.625	27.5625	26.6875
Height (North)		26.9375	27.8125	27.75	26.75
Stiffener Width (South)	8"	7.9375	7.9375	7.9375	7.9375
Stiffener Width (North)	8"	7.9375	7.9375	8	7.9375
Top Weld (South)	3/8"	7/8 (7/8)	3/4 (5/8)	5/8 (9/16)	7/8 (5/8)
Top Weld (North)	3/8"	3/4 (7/8)	3/4 (5/8)	5/8 (1/2)	3/4 (5/8)
Side Weld (South)	1/4"	1/4 (1/4)	1/4 (1/4)	1/4 (1/4)	1/4 (5/16)
Side Weld (North)	1/4"	1/4 (5/16)	1/4 (5/16)	5/16 (1/4)	1/4 (3/8)
Bottom Gap (South)	0	0.116	0.098	0.057	0.114
Bottom Gap (North)	0	0.085	0.077	0.142	0.266

1/4 (1/4) = East (West)

$$R_F = \frac{(0.06 + 0.72 (w / t_p))}{(t_p^{0.167})} \leq 1.0$$

w = the leg size of the reinforcing or contouring fillet in the direction of the thickness of the tension-loaded plate (in.).

t_p = thickness of tension loaded plate (in.).

Equation 2.2: Reduction factor of plates loaded in tension

When the dimensions that were detailed in the plans are used ($t_p = 0.6875$ inches, $w = 0.375$ inches), the reduction factor, R_F , equals 0.482. This cuts the design stress range for the weld on the stiffener in half lowering it from that of a category C detail, which is 10 ksi to around 5 ksi. When the values that were actually measured are inserted into the equation ($t_p = 0.625$ inches, $w = 0.75$ inches), the reduction factor equals 1.0 or in other words no reduction is applied. However, if the top of the stiffener is not flush with the continuity plate, the dimension w should be taken at the top of the stiffener, shown as w'' in Figure 2.14 and estimated as small as 0.32 inches in some of the details. A reduction factor of about 0.46 is calculated using $w = 0.32$ inches, which means the allowable stress range is closer to that of a category E instead of a category C detail.

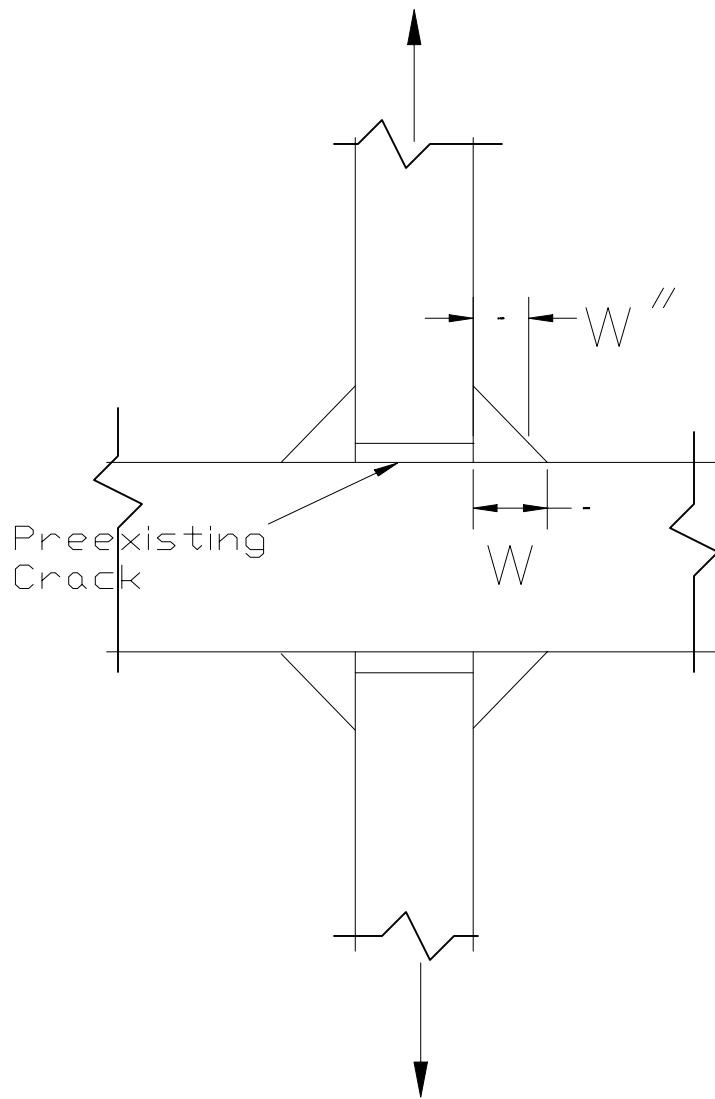


Figure 2.14: Crack-like notch between fillet welds in a cruciform connection

2.5 Mechanism for Fatigue Cracking

As vehicles travel across the bridge, their loads are distributed unequally over the girders. Due to this differential loading, the rotation of the girders at the pier caps also varies. When the girders are not allowed to move independently, as in the case when the girders run through the pier cap, forces are created resisting this differential movement. The girder end moments are transferred to the pier cap as torsion.

The continuity plate and the stiffeners transfer the forces from the girders to the pier cap, creating very high stresses in the stiffeners. The welds connecting the stiffeners become susceptible to fatigue under these high stresses. With multiple stiffener designs at the girder to pier cap intersection, the locations of the high stresses and the resulting cracking vary.

In Pier Cap 5, the intersection between the pier cap and girder can be broken into two cells. The top cell is contained between the top flange of the pier cap and the bottom flange of the girder. A 3/8" continuity plate representing the web of the girder fills this top cell and is welded on all edges. The bottom cell, found between the bottom flange of the girder and the bottom flange of the pier cap, consists of two 5/8" thick stiffeners 8" wide with an opening in between for access inside of the pier cap. Each of the stiffeners is welded to the bottom flange of the girder and the pier cap web, while it is milled to bear to the bottom flange of the pier cap.

Because of the opening of the lower cell, it is more flexible than the top cell of the pier cap, concentrating the distortion in the bottom cell as shown in Figure 2.15. Instead of remaining perpendicular with the girder as it rotates, the bottom flange of the pier cap is restrained by the supports at the piers. This causes the lower cell to shear, taking on the shape of a parallelogram. High stress ranges are created in the stiffeners as they resist this shearing.

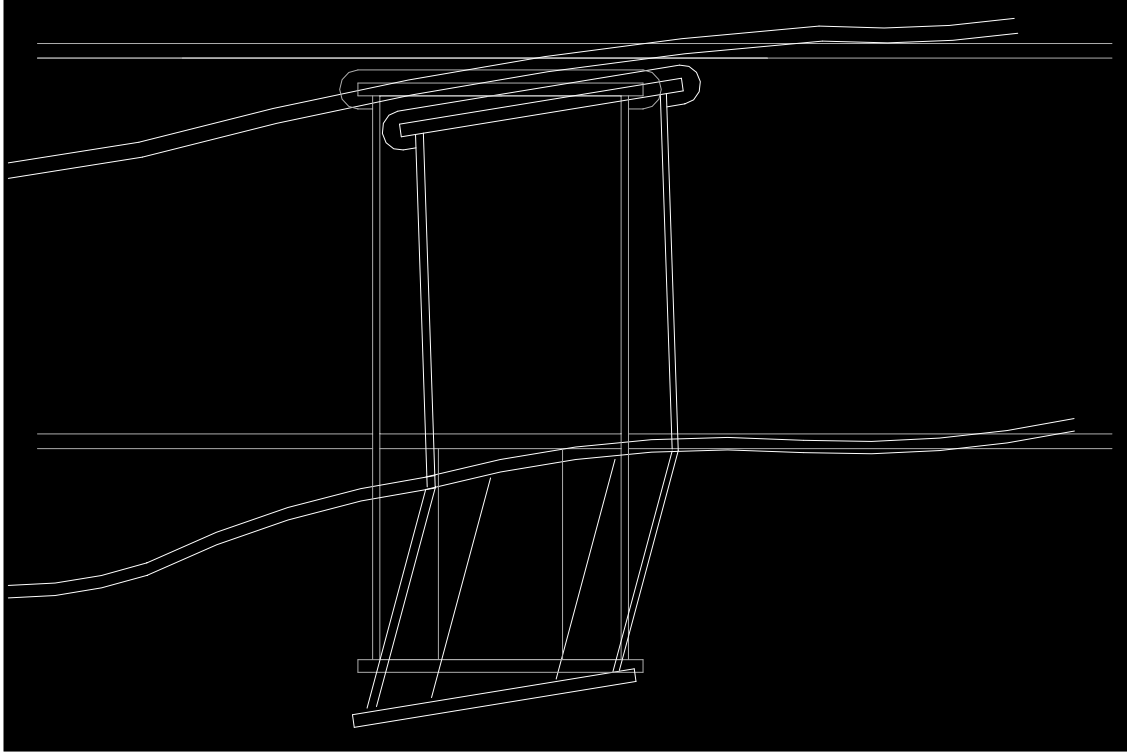


Figure 2.15: Exaggerated displaced shape showing concentration of distortion in lower cell

In order to confirm that this is the mechanism behind the high stress ranges taking place within the pier cap instrumentation of the bridge both globally and locally was performed. The next chapter explains the types of instruments used and their locations.

CHAPTER 3: FIELD INSTRUMENTATION AND TESTING

To determine how the bridge reacted to vehicle loadings several means of measurement were implemented on the girders and pier cap. A combination of strain gages, LVDTs (Linear Variable Differential Transformers), and inclinometers were used to determine the interaction between the pier cap and the intersecting girders.

Truck tests were performed on the bridge using Mn/DOT vehicles with known loads. This provided a standard for comparison to live traffic readings collected and for calibration of finite element models.

All readings from the instruments were recorded using a Campbell CS9000 Data Acquisition Systems and then transferred to a computer for analysis.

3.1 Instrumentation Plan

Instrumentation of Bridge 69832 used a variety of sensors and was completed in two different phases. Phase 1 focused on instrumentation of the girders and pier cap to monitor the overall reaction of the structure, while Phase 2 focused more locally on the interior of the pier cap. In total 71 weldable strain gages, 10 adhesive strain gages, four ½” GCD Series Gagehead LVDTs, four ¼” GCA Series Gagehead LVDTs, and two 14.5° inclinometers were used in the instrumentation of Pier cap 5 on Bridge 69832. Phase 1 was completed for the Mn/DOT truck tests, while Phase 2 was done at a later date. Live traffic data was collected from all instrumentation.

3.1.1 Phase 1 - Exterior Strain Gage, LVDT and Inclinometer Installation

Initial instrumentation involved the placement of 350-ohm weldable strain gages to all four girders and pier cap 5. A total of 71 strain gages were installed at this time. These gages were installed to obtain the nominal bending of each girder and the pier cap. The gages were also used for calibration of further data collection and of finite element models.

For installation of each gage, first the area was marked. Then the surface was ground smooth and cleared of paint. Next the area was cleaned of debris with a degreaser. Each gage was taped into place and then spot welded to attach it (Figure 3.1). Finally the gage was covered with caulking and duct tape to protect it from the environment.



Figure 3.1: Welding of a strain gage

For obtaining the strains due to bending in each girder, several gages were mounted at various cross-sections of the girder (Figure 3.2). On spans immediately adjacent to Pier Cap 5, three gages were placed at the midspans. One gage was located on the bottom flange, and the other two were spaced vertically along the web. Four gages were also placed in the negative moment region of each girder five feet from the center of the pier cap on both sides. One was placed on the bottom flange, and the other three were spaced through the web.

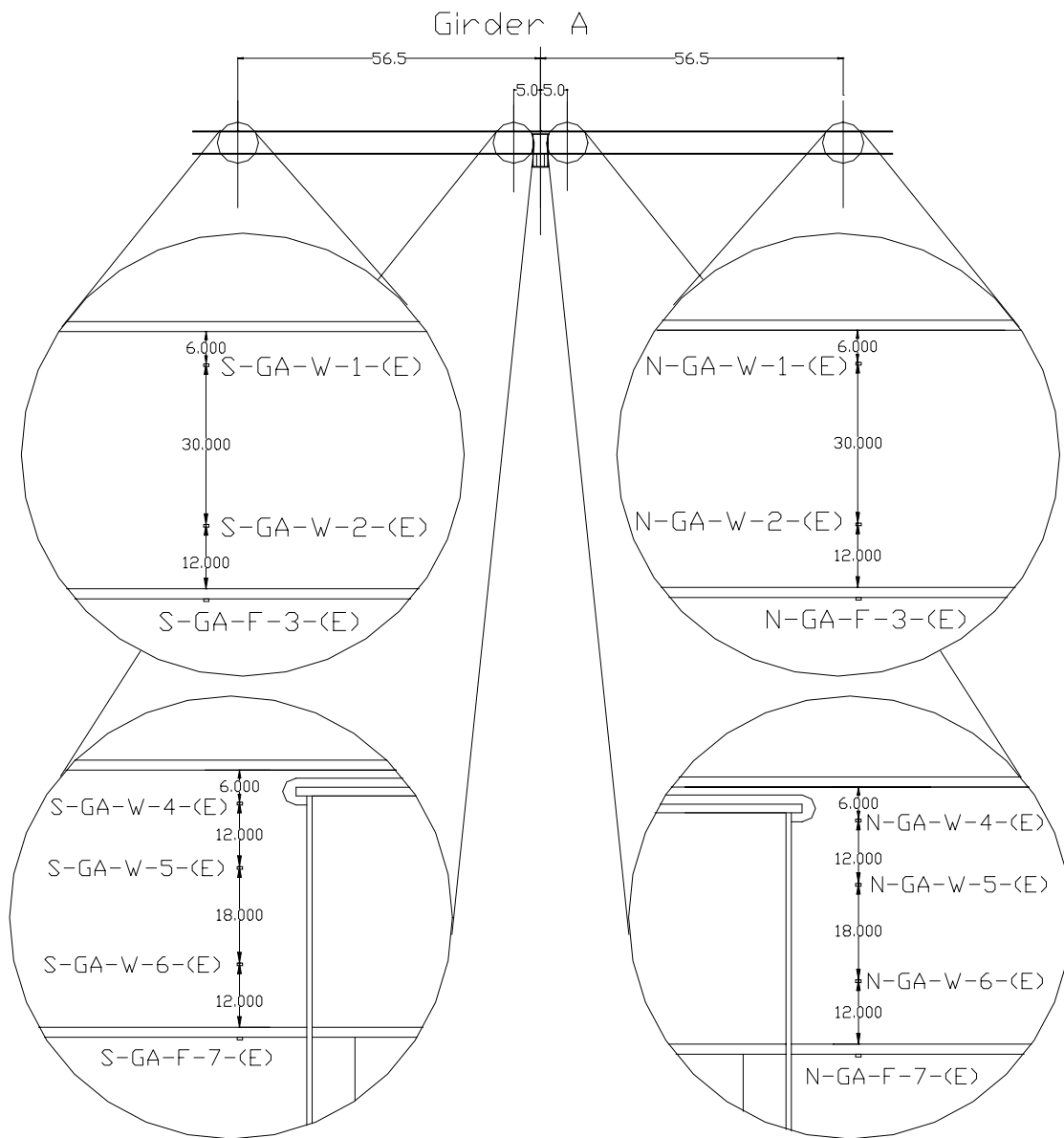


Figure 3.2: Girder A gage placement

Gages were also placed on the pier cap to obtain strains from bending (Figure 3.3). Gages were located midway between the two center Girders B and C, and midway between the West pier and Girder A. One gage was placed on the bottom flange at each location, and three gages were spaced vertically along the web on both sides of the pier cap. One gage was placed on the top flange at the location between Girder A and the pier.

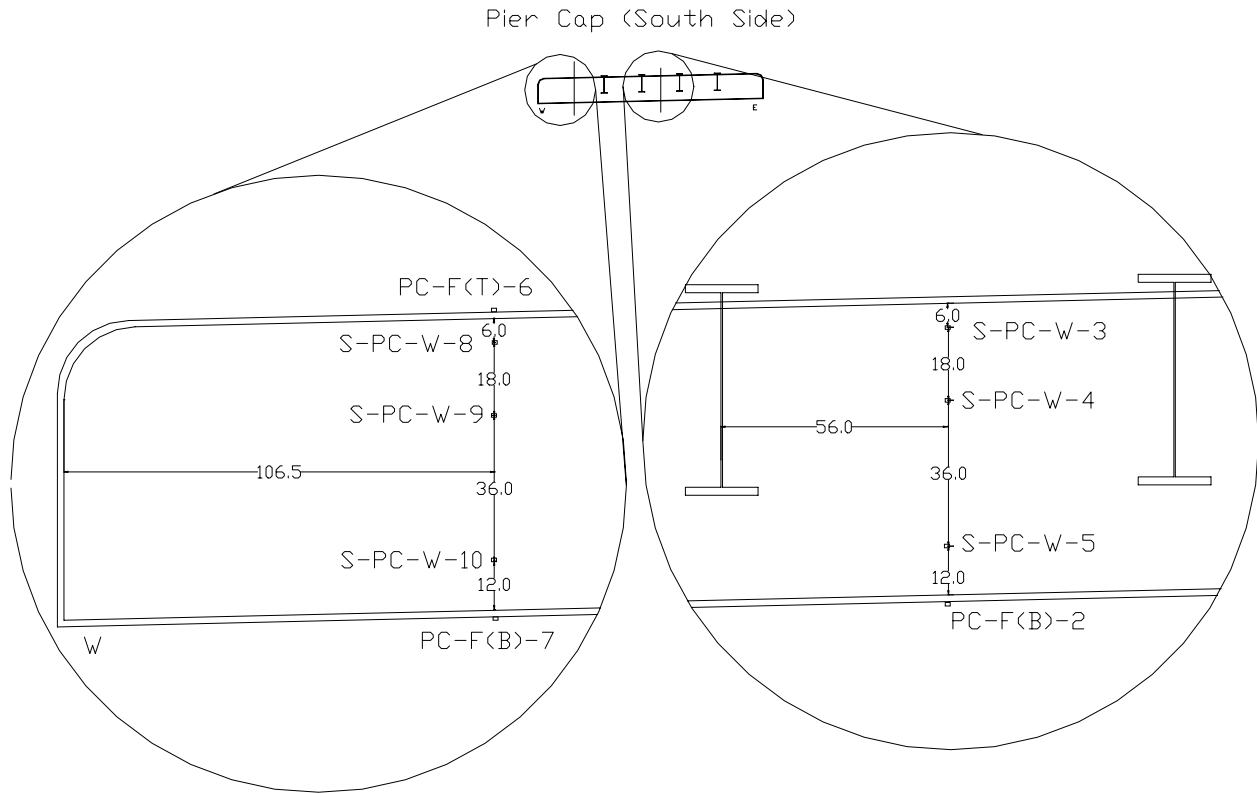


Figure 3.3: Pier cap gage placement

Labeling of the strain gages on the exterior of the bridge adhered to the following pattern. The first letter is either a S or an N indicating whether the gage is located on the South or the North side of the pier. The next set of letters tell which girder the gage is on, or if its on the pier cap. The letters GA would represent girder A, while the letters PC would indicate the gage is on the pier cap. The fourth letter is either a W or F, which informs whether the gage is located on the web or flange. If an F is followed by a B or T in parentheses it marks whether the gage is on the bottom or top flange. The number represents the gages position through the girder or pier cap. Lastly, an E or W in parentheses indicates whether the gage is on the East or West side of a girder.

To determine differential rotation between the pier cap and the girders, brackets were constructed to support LVDTs and inclinometers. The brackets were constructed of 1"x 1/8" square tubing, 1/4" plate, and 1 1/2"x 1 1/2"x 1/8" angle (Figure 3.4).

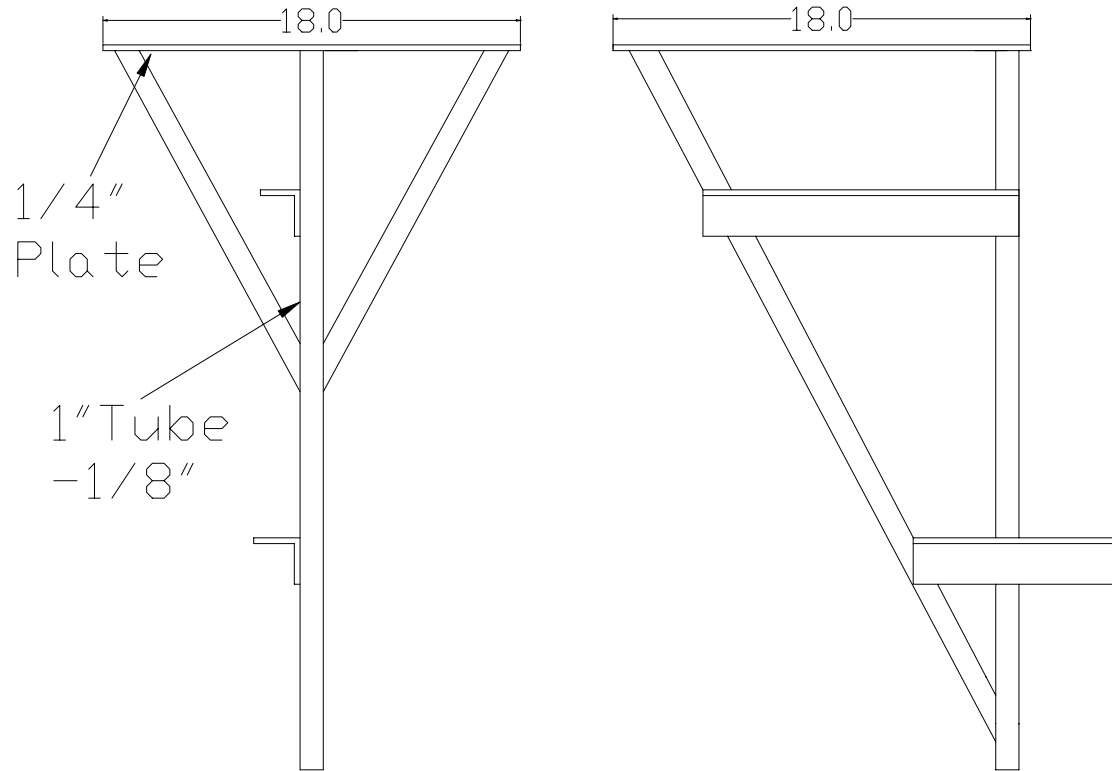


Figure 3.4: Bracket design plans

For instrumentation a bracket was C-clamped to the bottom flange of the girder (Figure 3.5). It was clamped approximately eight inches from the face of the pier cap. A 14.5° inclinometer was bolted to the upper angle for measuring the rotation of the girder. A $\frac{1}{2}$ " GCD Series Gagehead LVDT was clamped horizontally to the bracket and reached to the bottom flange of the pier cap. A $\frac{1}{4}$ " GCA Series Gagehead LVDT was clamped vertically to the lower angle and also reached to the bottom flange of the pier cap. The Gagehead LVDTs were used to measure the difference in rotation between the girder and the lower cell of the pier cap.

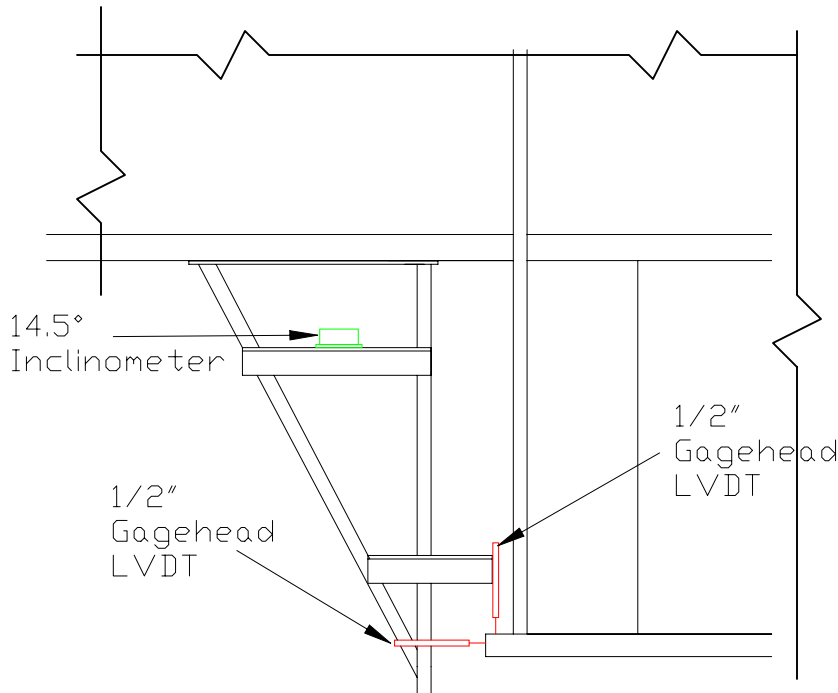


Figure 3.5: Installation of bracket

3.1.2 Phase 2 - Instrumentation of Pier Cap Interior

Additional instrumentation of Bridge 69832 was installed on the interior of Pier Cap 5. A combination of 350 ohm adhesive strain gages and 1/2" GCD Series LVDTs were used.

A total of 10 strain gages were installed. For installation the area was marked, ground smooth, and cleaned. Adhesive was then used to attach the gages to the area. Once dry, caulking and duct tape were applied to protect the area from the environment.

The strain gages were located on each uncracked stiffener between the bottom flange of the girder and the bottom flange of the pier cap (Figure 3.6). The south stiffeners on girders A, B, C, and D, and the north stiffener on girder D were instrumented. Two gages were placed vertically on each stiffener to measure the tensile strains as the stiffener is pulled away from the flange of the girder. The gages were placed at the toe of the horizontal weld connecting the stiffener to the bottom flange of a girder. One gage was located 1" from the edge of the stiffener. The other gage was located 2.5" from the web of the pier cap. The strain gages were used to measure the magnitude of the hot spot strains in the stiffeners. Adhesive strain gages were used instead of weldable strain gages in order to place the strain gage as close to the weld toe as possible.

In labeling the gages the first letter represented the girder. The number represented the strain gage position, a 1 is if the gage is located 2.5" from the web of the pier cap and a 2 is used

for the gages located 1" from the edge of the stiffener. The last letter indicated whether the gage was on the North or the South stiffener.

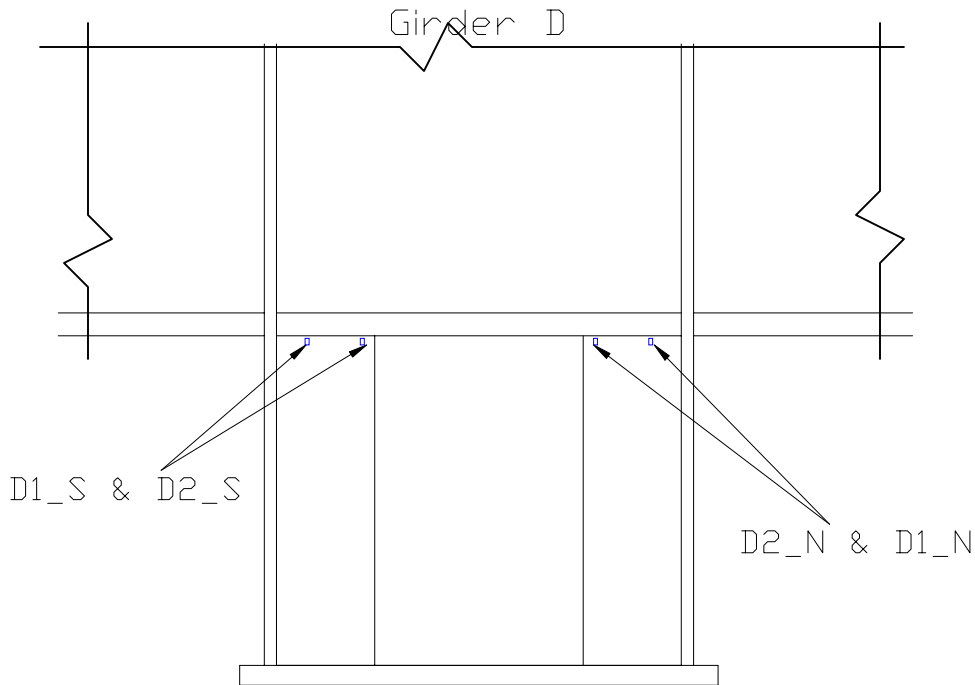


Figure 3.6: Interior of Pier Cap 5 gage placement Girder D

After the strain gages were mounted, two ½" GCD Series Gagehead LVDTs were installed inside the pier cap. Because of the limited number of LVDTs, two LVDTs were iterated through eight different positions at each girder intersection (Figure 3.7). Positions 1 and 2 measured shearing of the top cell of the pier cap by recording any changes in the length of the diagonal. Positions 3 and 4 measured shearing of the lower cell. Positions 5 and 6 measured the gap opening between the stiffener and the bottom flange of the pier cap. Positions 7 and 8 measured shearing of the pier cap at the intermediate stiffeners.

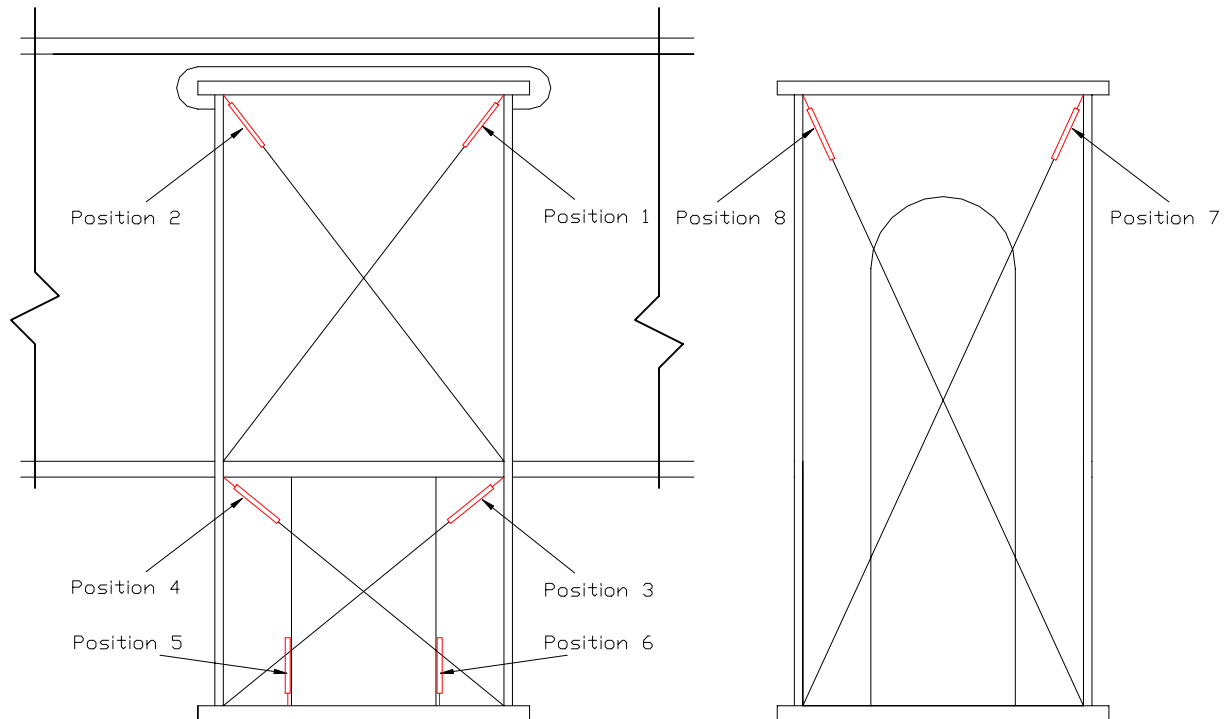


Figure 3.7: Interior of Pier Cap 5 LVDT placement

To attach the LVDTs 1”x1”x1/8” angles were used. The angles were attached diagonally and c-clamped at the lower corner. The LVDT was clamped to the other end of the angle and reached to the upper corner.

3.2 Test Descriptions and Data Retrieval

The following gives descriptions of the equipment used and the procedures taken during the truck tests. A description of the instruments used for reading and recording the data from the truck tests and the further live traffic data is also included.

3.2.1 Mn/DOT Truck Test Descriptions

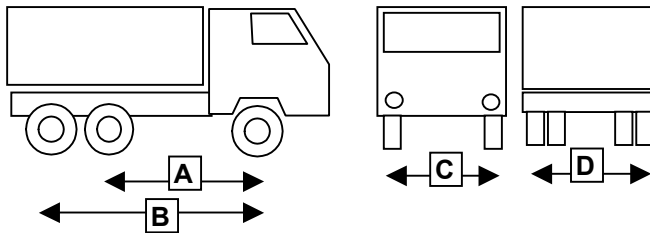
For comparison with live traffic data and for calibration of finite element models, a truck test was performed on Bridge 69832. Four three-axle Mn/DOT trucks were used for the test (Figure 3.8). Each truck weighed approximately 50 kips. The front axle carried approximately 28% of the total weight while the second and third axle both carried approximately 36% of the total weight. Table 3.1 gives the exact weights and dimensions of each truck.



Figure 3.8: Mn/DOT three-axle truck

Table 3.1: Mn/DOT truck weights and dimensions

Truck #	92073	88048	93198	93202
Total Weight (lbs)	50150	50100	49800	49800
1st Axle	13450	11400	14150	13150
2nd Axle	18100	19250	18200	18250
3rd Axle	18600	19450	17450	18400
Truck Dimensions				
A	14' 8"	13' 1"	14' 5"	15'
B	19' 4"	17' 9"	19' 1"	19' 3"
C	6' 8"	6' 5"	6' 9"	6' 8"
D	6' 2"	6'	6' 2"	6' 2"



The first four truck tests had varying formations at approximately 5-10 mph. Due to these speeds a momentary full closure of the bridge was done for each pass. Upon completion of each test, traffic was opened again. The next test was then performed once traffic had decongested.

In the first pass the four trucks ran in a 2x2 formation (Figure 3.9). The trucks followed the car lanes with spacing at a minimum between trucks. The trucks traveled at 5-10 mph keeping the formation through pier 7.

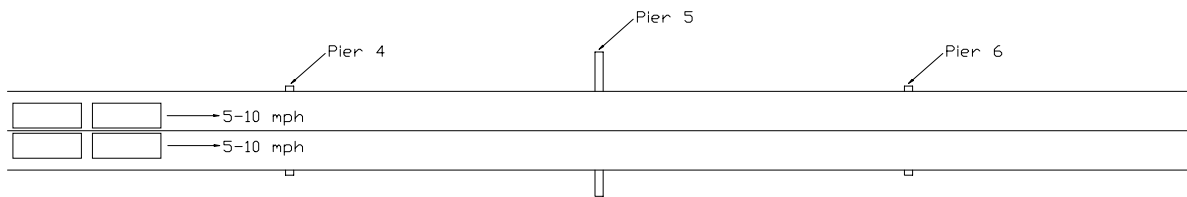


Figure 3.9: Truck Test 1

Truck test #2 was split into two parts. First two trucks traveled in the left lane at 5-10 mph with spacing as close as possible. Once the first two trucks had cleared pier 7, the second two trucks traveled in the right lane at 5-10 mph with spacing as close as possible (Figure 3.10).

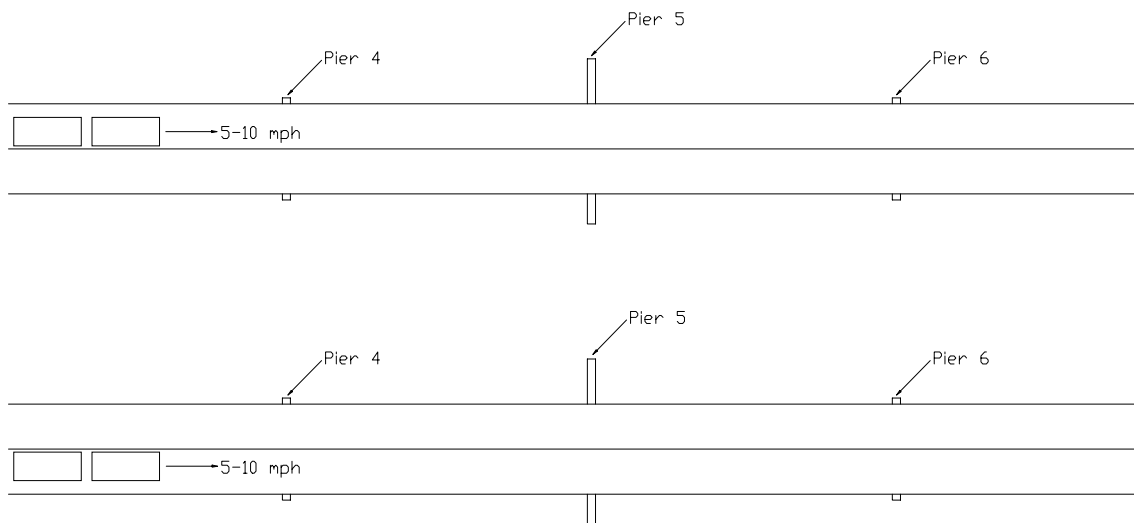


Figure 3.10: Truck Test 2

Truck Test #3 had two trucks in the left lane and two trucks in the right. Approximately 1 span (110 ft) was kept between each set of trucks (Figure 3.11). The trucks traveled across keeping the same distance apart at 5-10 mph.

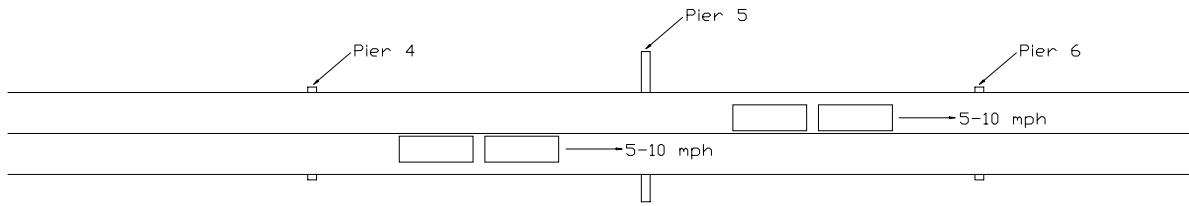


Figure 3.11: Truck Test 3

Truck Test #4 was a repeat of Truck Test #1 (Figure 3.12).

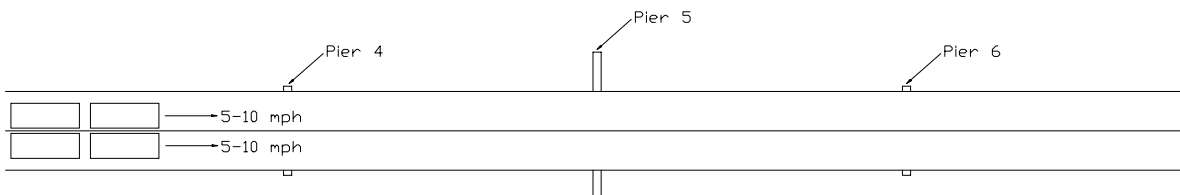


Figure 3.12: Truck Test 4

Fig

Upon completion of Truck Tests #1-4, both lanes were opened to traffic. Each truck then took multiple passes at 55mph with live traffic.

At a previous date a Mn/DOT snoop truck was also used in a truck test. It traveled at approximately 5mph in the right lane. The truck weight of the snoop truck was 63.4 kips, with 28% in the front axle, 60% in the two drive axles, and 12% in the tag axle.

3.2.2 Live Traffic Monitoring

On multiple occasions live traffic monitoring took place. Prior to the truck tests live traffic readings were taken to check the instruments for noise levels and for their effectiveness in giving pertinent information.

After the completion of the truck tests, further instrumentation of the interior of the pier cap took place (Section 3.1.2). All data collected from these instruments was from live traffic. These readings were then correlated to those from the truck tests to determine the approximate loadings.

3.2.3 Data Collection

Two Campbell PC9000 data acquisition systems were used for reading the sensors (Figure 3.13). Data was collected at a rate of 66.7 Hz (a sample every 0.015 seconds). A combination of $\frac{1}{4}$ bridge circuits (the strain gages) and voltage differentials (the LVDTs and inclinometers) were monitored.



Figure 3.13: PC9000 data acquisition system

All the gages were monitored for live traffic data prior to the truck test to make sure they were working and to see how much of a problem noise would be. Steps were taken to reduce the noise as much as possible but some gages still had high noise levels or were defective. These gages were disregarded in the analysis for there was enough redundancy in the locations of the gages installed. Reasons for the defective gages include damage during installation and/or faulty wiring.

The inclinometers proved to be too sensitive for any high-speed tests. Vibrations due to traffic made it impossible to decipher any readings from these. Only during the truck tests at very low speeds was it possible to get legitimate readings from the inclinometers, even then their outputs were very noisy.

The DC gagehead LVDTs were the most effective instrument for taking measurements. The LVDTs were stiff enough to not be affected by the vibrations of the bridge and very little noise was detected in them. It was possible to take readings down to the ten-thousandth of an inch. The AC LVDTs had higher noise levels and weren't as effective.

CHAPTER 4: DATA ANALYSIS FROM FIELD INSTRUMENTATION

Data were collected during several different periods on the bridge. Initial readings were taken on the exterior strain gages and a test bracket rigged with LVDTs and inclinometers. These readings were taken to test the gages and to evaluate the effectiveness of the brackets. The only known load to go over during this time was the snooper that was being used for inspecting the bridge.

After the brackets were proven useful, four were installed for the truck tests. During the truck tests readings were recorded from the exterior strain gages and the LVDTs and inclinometers on the brackets. The tests used four 50-kip Mn/DOT trucks in various patterns. This gave known loads, which could then be correlated to further live traffic data for analysis.

The final stage of data collection was the recording of readings from inside the pier cap. Essential exterior strain gages and one LVDT bracket were recorded simultaneously with the gages and LVDTs inside the pier cap. Thus it was possible to decipher the size of the load traveling over the bridge.

This chapter analyzes the readings that were recorded during the truck tests and from live traffic.

4.1 Truck Test Results

A summary of the readings obtained from the sensors from each of the truck tests is covered, along with readings from live traffic.

4.1.1 Test 1

Truck test 1 consisted of four trucks in a 2x2 pattern crossing over the bridge (Section 3.2.1). This gave a maximum load that was distributed over all four girders.

The load distributed fairly evenly over the four girders during this test (Figure 4.1). This plot shows the strains ($\times 10^{-6}$) in the gages located on the bottom flange of the girders at midspan. It is also shown that the reactions are more or less symmetric between the north and south spans.

Figure 4.2 shows that the girders were working compositely with the concrete deck. All three gages through the depth of the girder go into tension when a load passes over indicating the neutral axis is located near the top flange. The gages are located at the bottom flange, 12 inches up from the bottom flange on the web, and 6 inches down from the top flange on the web (Section 3.1.1).

Figure 4.3 shows the readings from the horizontal LVDTs attached to the brackets. This indicates that there is a differential movement between the girders and the pier cap (Section 2.5). The exterior girders show slightly higher maximum readings than the interior girders. This is due to the piers resisting the movement of the bottom flange of the pier cap. At the interior

girders the bottom flange is not as restricted and the lower cell moves with the girder. This would lead to smaller stresses occurring in the interior girders, since less shearing is taking place.

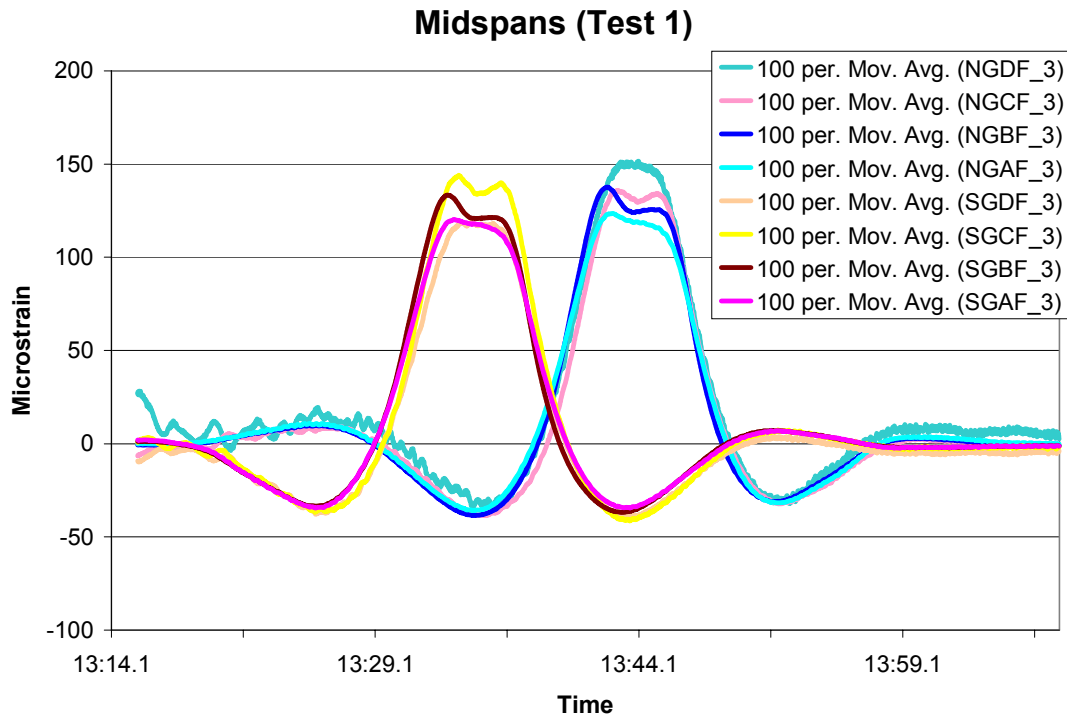


Figure 4.1: Strain gage readings from midspan locations during Test 1

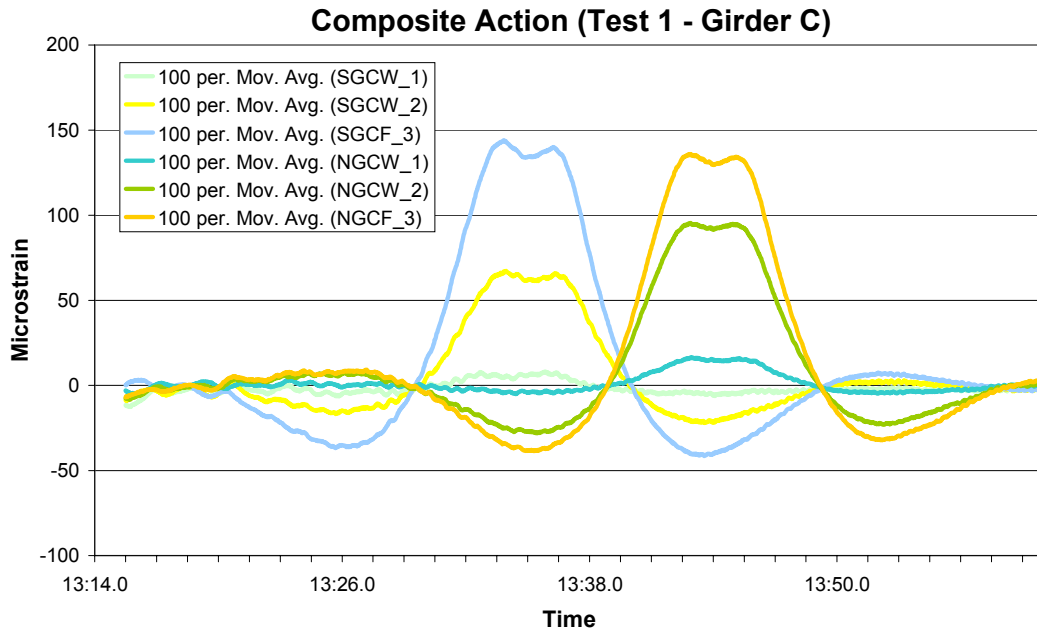


Figure 4.2: Composite action from midspan of Girder C

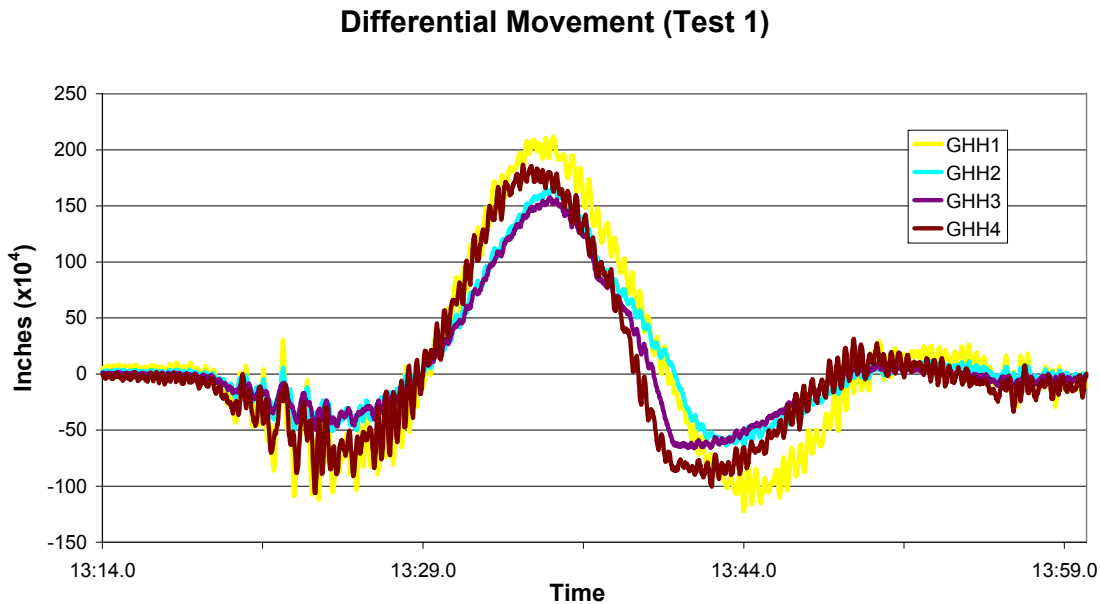


Figure 4.3: Horizontal LVDT readings showing differential movement of girders (Test 1)

4.1.2 Test 2

Truck Test 2 consisted of two passes, the first in the right lane and the second in the left. Each pass consisted of two trucks with one following behind the other (Section 3.2.1).

The load distribution for a vehicle in one lane is shown in Figure 4.4. The two girders that the vehicle was located over carry approximately equal amounts, around 35% of the vehicle load. The next girder over carries around 20% and the furthest away from the load carries around 10% of the load. This is approximately the same, regardless of which lane the vehicle is in.

The differential movement shows that the exterior girder nearest the load undergoes the largest deformation (Figure 4.5). The other girders then decrease in the movement, with the opposite exterior girder showing a negative value. The pier cap is caused to twist from the load on the other girders, but the opposite exterior girder does not rotate enough to match this twisting of the pier cap. Thus it is resisting the rotation of the pier cap.

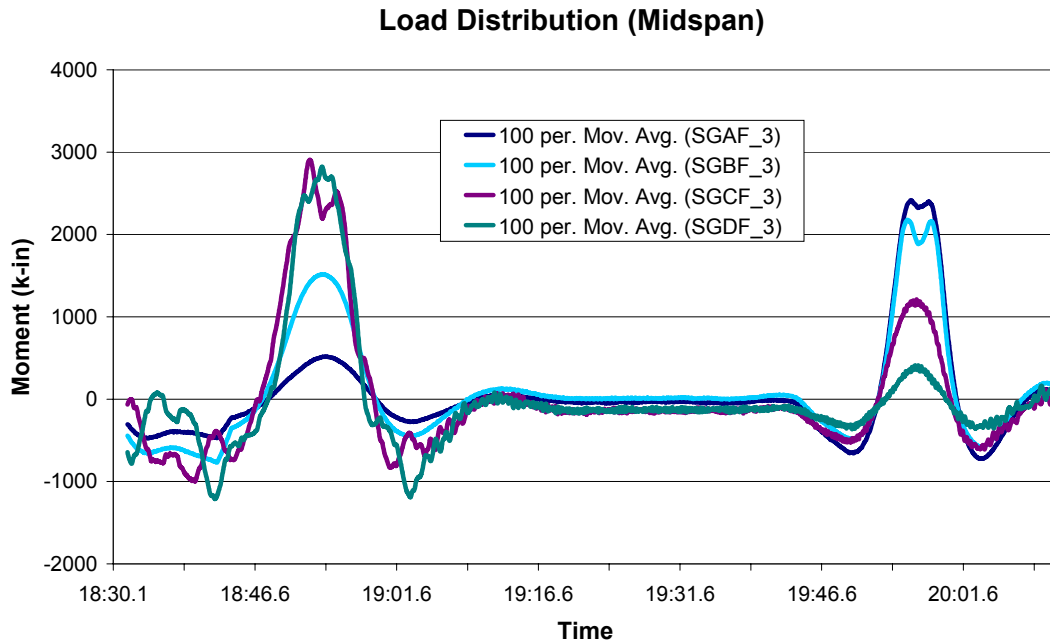


Figure 4.4: Load distribution among the girders during Test 2

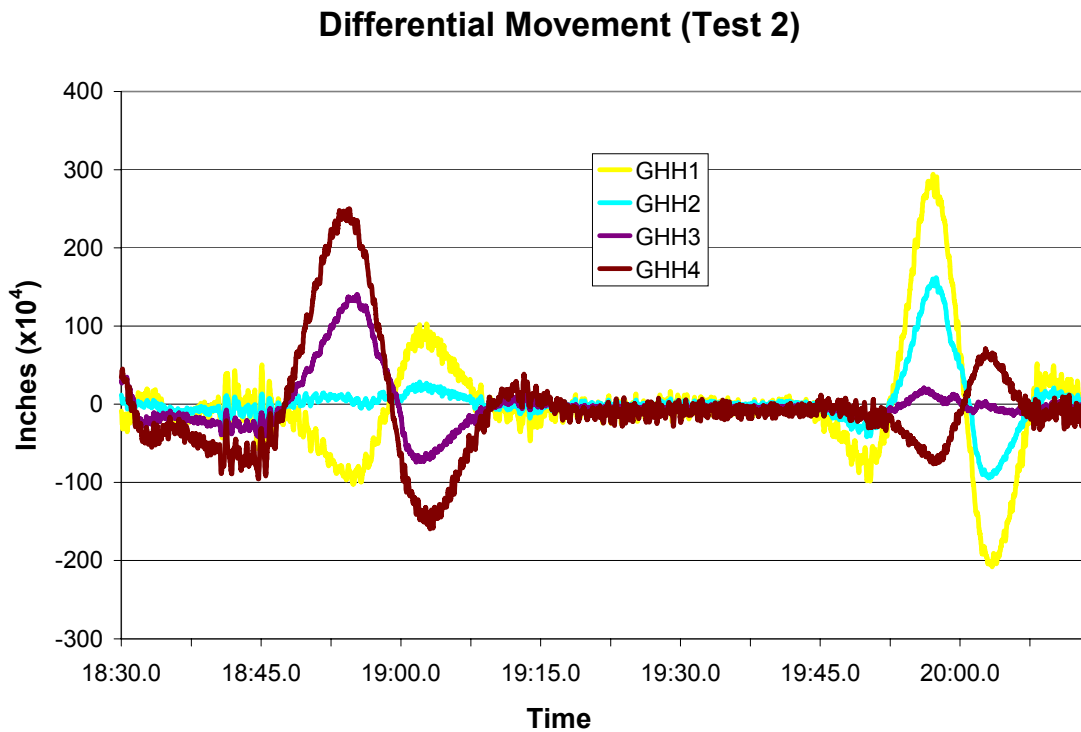


Figure 4.5: Horizontal LVDT readings showing differential movement of girders (Test 2)

4.1.3 Test 3

Truck Test 3 consisted of having two trucks in each lane, with one span length between the two sets of trucks. This was to try to obtain the largest torque in the bridge.

Truck Test 3 did not provide a large amount of useful data (Figure 4.6 & Figure 4.7). With the over lapping of the loads it was difficult to decipher the components of the values.

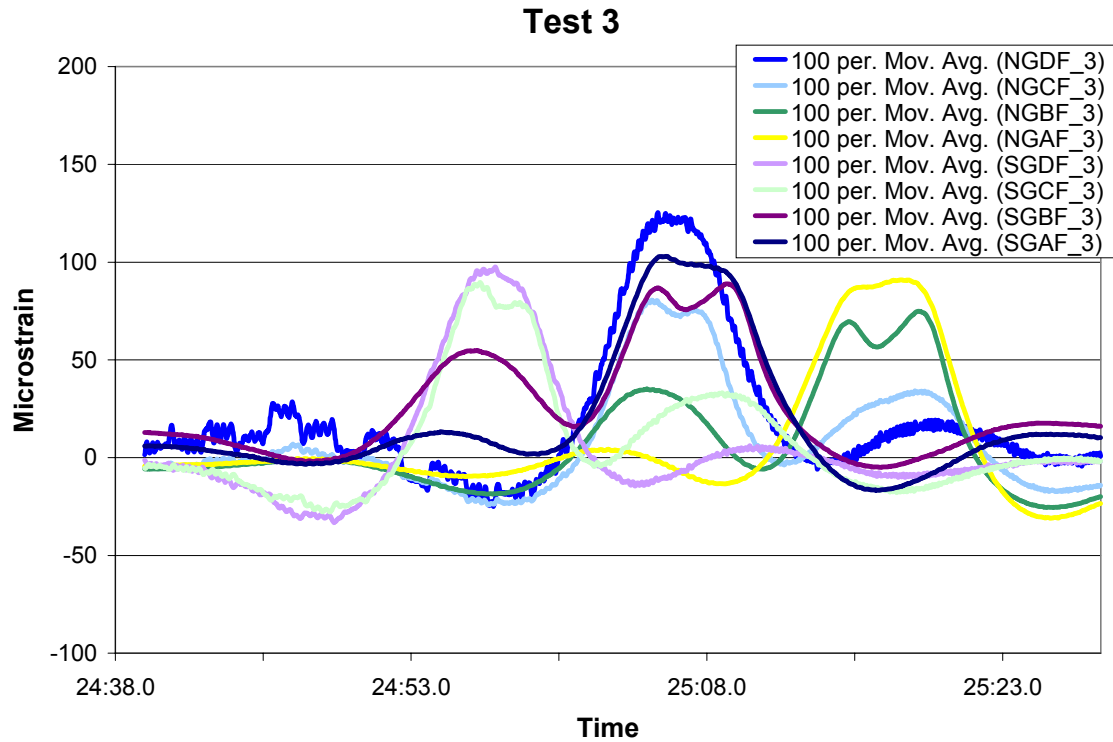


Figure 4.6: Strain gage readings from midspan locations during Test 3

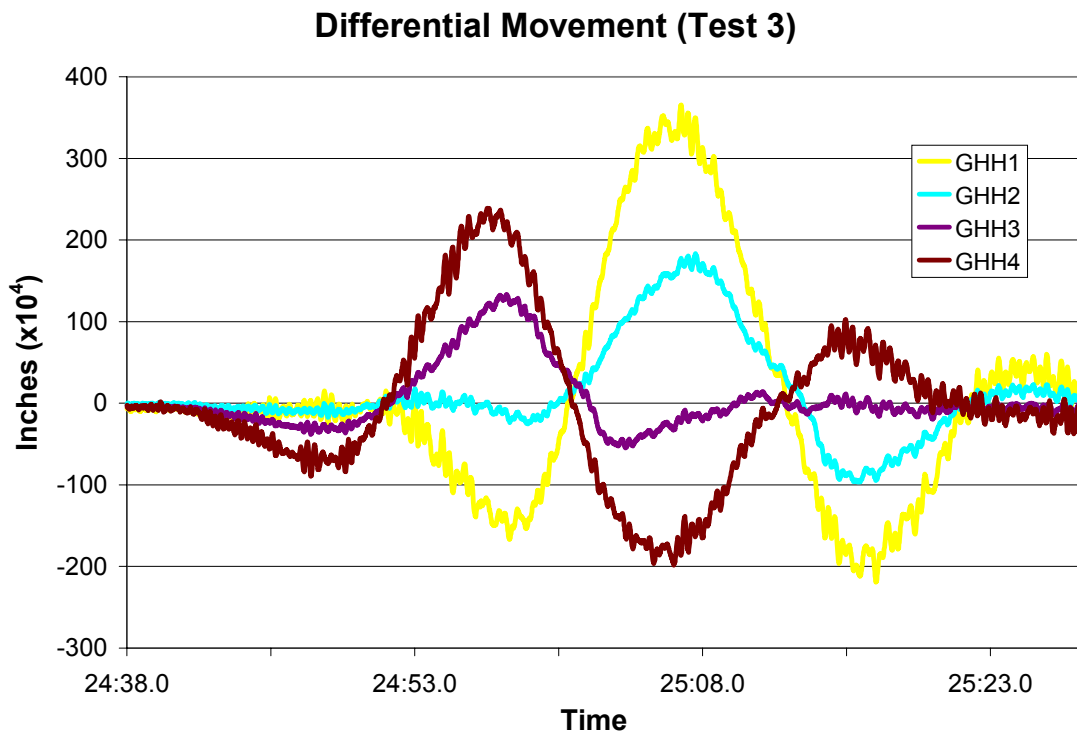


Figure 4.7: Horizontal LVDT readings showing differential movement of girders (Test 3)

4.1.4 Test 4

Truck Test 4 was equivalent to Truck Test 1. Its main purpose was to confirm the repeatability of the tests, which was confirmed.

4.1.5 Additional Testing

After the initial 4 truck tests, several passes were made of single trucks at regular traffic speeds. These produced reactions similar to Truck Test 2.

As noted above, at a previous date the snoopers were recorded going over the bridge. It was the only pass by a vehicle that produced readable data for the inclinometers. All other passes proved to be too noisy to decipher any legitimate data. The inclinometers were located on girders C and D for the snoopers test. As the plot shows the results were still very noisy (Figure 4.8).

Inclinometer (Snooper)

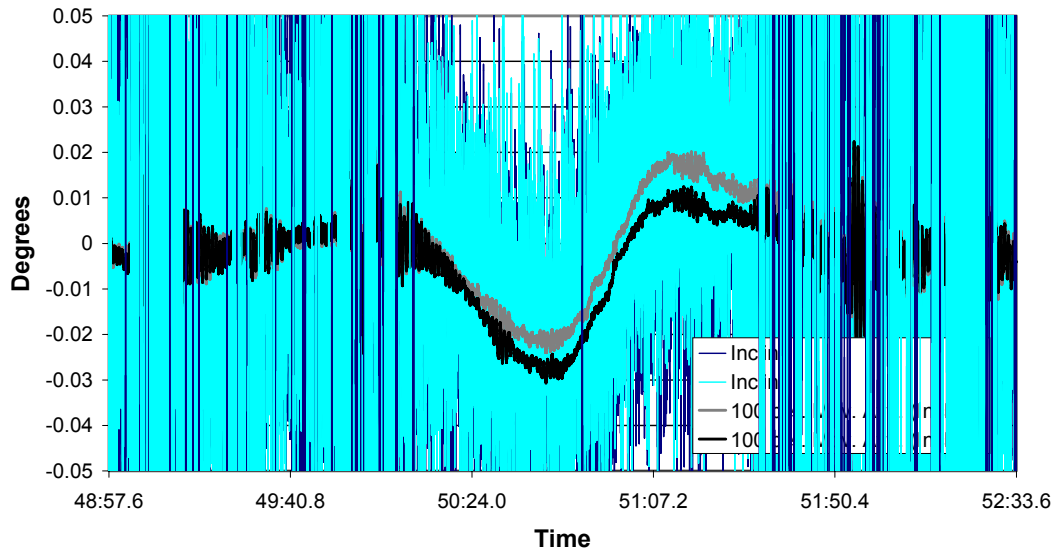


Figure 4.8: Inclinometer readings from Mn/DOT Snooper

After the completion of all the truck tests, the readings at significant gage locations were recorded and summarized (Table 4.1). Cells with no values were either too noisy to read or were not recorded. From these results plots were created showing the linearity in the applied loads (Figure 4.9 & Figure 4.10). The plots were then used for correlating future live traffic data and determining the approximate vehicle loads. The values from the horizontal LVDTs showed the greatest linearity, and were the most essential in determining the loads. The gages were not as linear, but this is due to the gages being noisier than the LVDTs making accurate readings difficult.

Table 4.1: Truck Test results summary

		Snooper [R]	50-kip [R]	2x50-kip [R]	50-kip [L]	2x50-kip [L]	4x50-kip
Midspan (microstrain)	Gir A - S		15.33	29.00	77.75	109.00	134.50
	Gir B - S	29.00	39.33	69.00	71.25	100.00	154.50
	Gir C - S	82.00	74.7	106.00	39.25	44.00	156.50
	Gir D - S	118.00	69.80	115.00	16.00	22.00	126.50
	Gir A - N		16.90	23.00	89.75	110.00	134.50
	Gir B - N	29.00	41.33	55.00	77.00	92.00	152.50
	Gir C - N	85.00	73.57	95.00	36.50	49.00	146.50
	Gir D - N	135.00	77.43	140.00	15.25	28.00	152.00
Negative Moment (microstrain)	Gir A - S	0.00			-11.18	-13.00	-17.00
	Gir B - S	-6.50		-17.50	-16.40	-29.50	-41.00
	Gir C - S	-16.00	-10.50	-16.00			-26.50
	Gir D - S	-26.50	-12.83	-24.00			-30.00
	Gir A - N			-4.50	-14.69	-21.50	-25.00
	Gir B - N	-4.00		-10.50	-10.63	-19.00	-26.25
	Gir C - N		-8.50	-13.00			-19.00
	Gir D - N	-35.50	-15.67				-29.50
Horizontal LVDT (Inches x10 ⁴)	Gir A - S		-42.33	-88.00	182.25	283.00	221.00
	Gir B - S		17.67	11.00	101.00	157.00	178.00
	Gir C - S	95.00	76.33	136.00	14.75	17.00	159.00
	Gir D - S	168.00	123.67	244.00	-45.75	-71.00	180.00

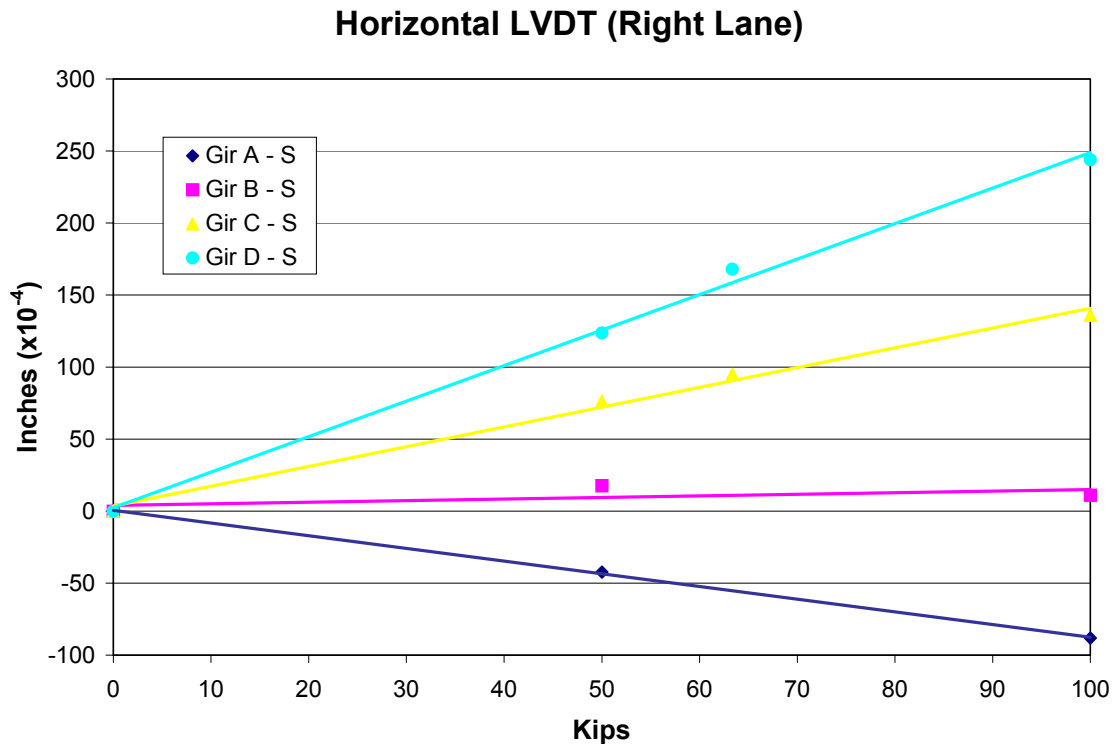


Figure 4.9: Linear interpolation of horizontal LVDT data for a vehicle in right lane

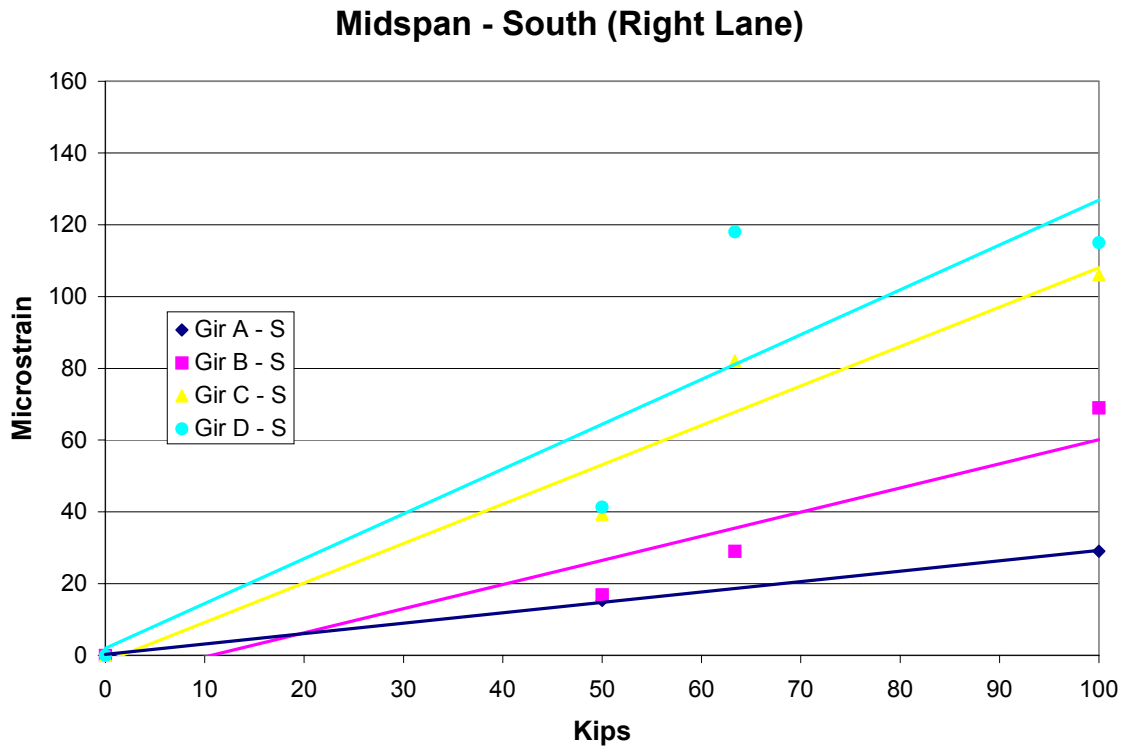


Figure 4.10: Linear interpolation of midspan strain gage data for a vehicle in right lane

4.2 Live Traffic Analysis

After completion of the truck tests, the second phase of instrumentation was conducted on interior of the pier cap. Strain gages were placed at the toe of the welds on the stiffeners in the lower cell of the pier cap. LVDTs were also iterated through various positions throughout the pier cap. The results were then correlated to the truck test results to determine loading.

Figure 4.11 shows the typical reaction of the strains in the stiffeners for a vehicle traveling in the right lane. These readings correspond with the movement determined from the horizontal LVDTs for a vehicle traveling in the right lane during the truck tests. The highest strain recorded from the strain gages was $450\mu\epsilon$ located on the North stiffener at girder D. This equated to approximately a 105 kip load in the right lane. This strain translates to an approximate stress range of 13 ksi, higher than the CAFL of 10 ksi for a type C detail.

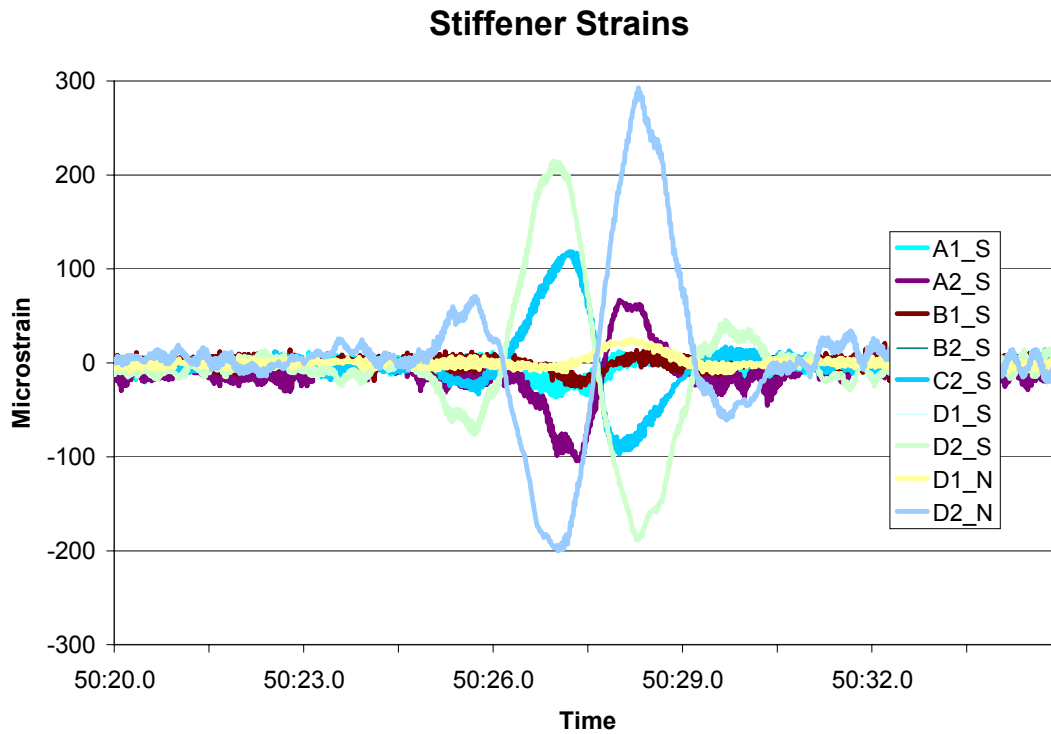


Figure 4.11: Stiffener strains from interior of pier cap

To confirm the shearing of the lower cell of the pier cap, LVDTs were placed diagonally across the cells. Positions 1 & 2 were in the top cell and positions 3 & 4 were in the bottom cell. As the cell shears it takes the shape of a parallelogram and the length of the diagonals change. Figure 4.12 demonstrates this taking place. Very little deformation took place in the top cell compared to the bottom cell. This is due to there being an opening in the lower cell, creating a softer story compared to a full continuity plate in the top cell making it much more rigid.

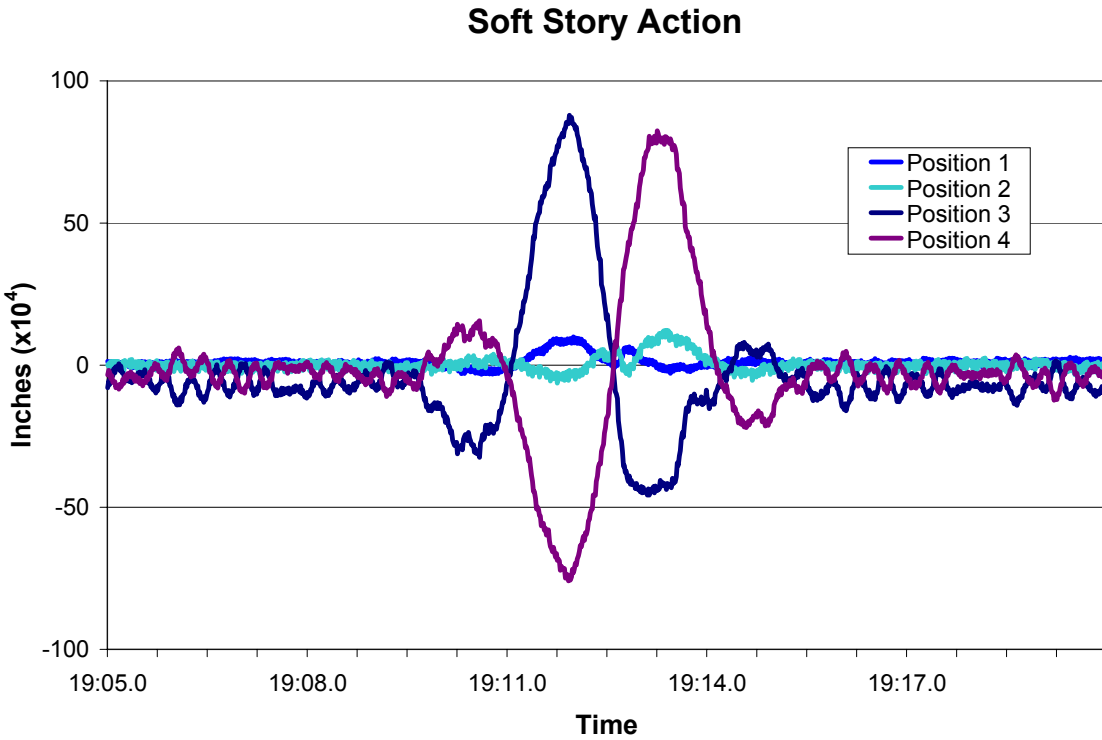


Figure 4.12: Shearing of the top and bottom cells

Since all readings from the pier cap were taken on live traffic only, the results were correlated with values from known loads. By interpolating the strains on the plots showing the linear relationship of the loads from the truck tests made it possible to approximate the load of the vehicle crossing the bridge. Table 4.2 shows what the approximate values would be from each of the instruments located inside the pier cap for a theoretical 50 kip truck in the right lane.

Table 4.2: Readings for a typical 50-kip truck

Typical 50-kip Truck Right Lane				
Midspan	(microstrain)		LVDT interior PC	(inches x10 ⁴)
Gir A - S	14.50	Gir A	Pos 1	5.35
Gir A - N	13.00		Pos 2	5.35
Gir B - S	32.00		Pos 3	15.20
Gir B - N	29.50		Pos 4	32.67
Gir C - S	61.50		Pos 5	10.94
Gir C - N	59.00		Pos 6	12.50
Gir D - S	72.00	Gir B	Pos 1	3.45
Gir D - N	85.00		Pos 2	2.88
Horizontal LVDT	(inches x10 ⁴)		Pos 3	14.39
Gir A - S	-43.00		Pos 4	10.61
Gir B - S	10.00		Pos 5	3.55
Gir C - S	72.00		Pos 6	0.96
Gir D - S	125.00	Gir C	Pos 1	0.74
Stiffener Strains	(microstrain)		Pos 2	0.00
Gir A	-49.45		Pos 3	40.86
Gir B			Pos 4	40.58
Gir C	59.28		Pos 5	5.03
Gir D - S	133.56		Pos 6	11.20
Gir D - N	160.52	Gir D	Pos 1	6.59
			Pos 2	7.58
			Pos 3	54.61
			Pos 4	56.66
			Pos 5	20.06
			Pos 6	16.62

From the live traffic data that was collected a rain-flow count was also done. This was conducted to provide information on the distribution of the vehicles that load Bridge 69832. The rain-flow count was performed on the strain gage located on the bottom flange on Girder C at midspan, gage S-GC-F-3 (W). This gage was monitored to provide information on vehicles traveling mainly in the right lane of traffic.

A lower bound value of 0.4 ksi was set to avoid counting cycles due to noise and smaller vehicles. This cutoff is equivalent to approximately a 10 kip truck traveling over the bridge, so all smaller vehicles were ignored as the magnitude of these cycles are insignificant to the fatigue life of the details.

The live traffic used was collected from several different periods over the summer. Each set of data contained approximately 2-3 hours of monitoring, no long-term monitoring was conducted in the collection of data.

Table 4.3 shows the number of events recorded that exceeded each given stress level and the numbers of events within each stress range. Approximately half the cycles recorded fell below the 1.0 ksi range. Figure 4.13 also shows these results. This indicates that the majority of the truck traffic was below 30 kips if the vehicles were traveling in the right lane. Results also show that more events happened in the 2.0-2.5 ksi range than in the 1.5-2.0 ksi range.

Table 4.3: Number of events exceeding each stress level for gage S-GC-F-3 (W)

Stress (ksi)	# of Cycles Exceeding	# of Cycles per Range	% of Total
0.4	1305	592	45.36%
1.0	675	261	20.00%
1.5	385	96	7.36%
2.0	277	161	12.34%
2.5	101	98	7.51%
Time (seconds)	36200		

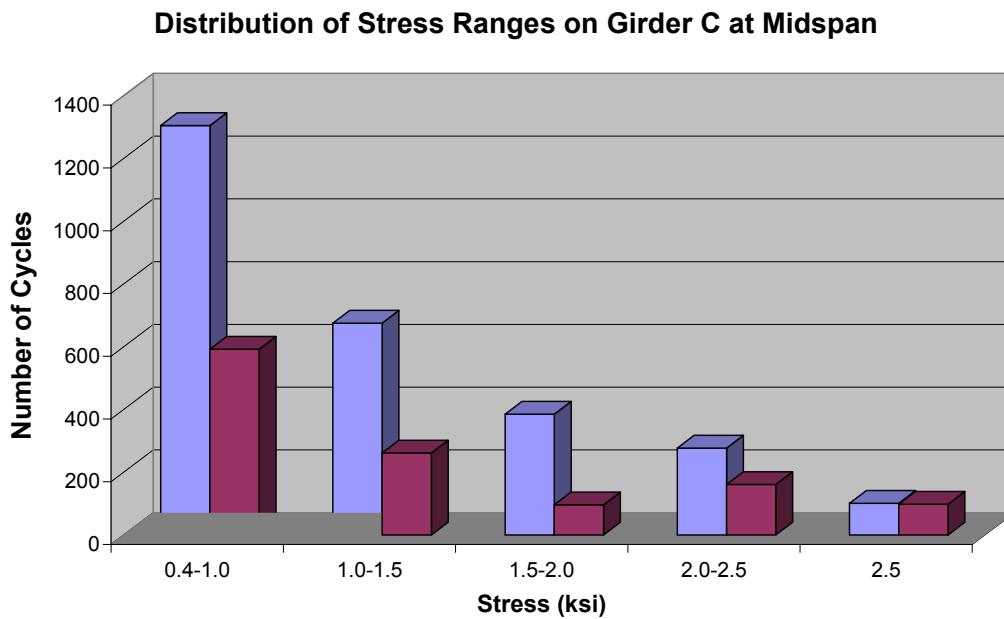


Figure 4.13: Stress range distribution for gage S-GC-F-3 (W)

For a 24-hour day, approximately 3100 events can be expected to occur on bridge 69832. Since these events are of varying amplitude, they cannot be assessed with the S-N curves that are based on constant amplitude. To account for this Miner's rule is applied to calculate an equivalent constant-amplitude stress range (S_{reff}) as in Equation 4.1 (7):

$$S_{\text{reff}} = (\sum p_i S_{ri}^3)^{1/3}$$

where: p_i = fraction of stress ranges in a particular interval i
 S_{ri} = mean stress range for interval i

Equation 4.1: Miner's Rule

When this equation is applied to the data in Figure 4.13 the equivalent stress range is 1.38 ksi.

From the analysis of the data collected from the truck tests and live traffic, comparisons can be made to finite element models representing Bridge 69832. These models are discussed in the following chapter.

CHAPTER 5: FINITE ELEMENT MODELING AND ANALYSIS

For further analysis of Bridge 69832, finite element models were created using SAP 2000. A three-dimensional grillage model was created modeling the 4-span continuous section containing pier cap 5. This was used to evaluate the overall performance of the bridge, and was used for analyzing moving load cases. Models were also created using shell elements to represent the pier cap. These allowed for more in-depth analysis of Pier Cap 5 and the areas of high stress concentrations. Three models of this type were created. The first model represented the uncracked pier cap, the second modeled the stiffeners completely cracked through, while the third represented a retrofit of the pier cap.

5.1 Three-dimensional Grillage Model

To understand the forces in the bridge and its overall behavior due to vehicle loading a three-dimensional grillage model was created using SAP 2000. The 4-span continuous section with Pier Cap 5 at the center was modeled. All components of the bridge were composed of frame elements (Figure 5.1).

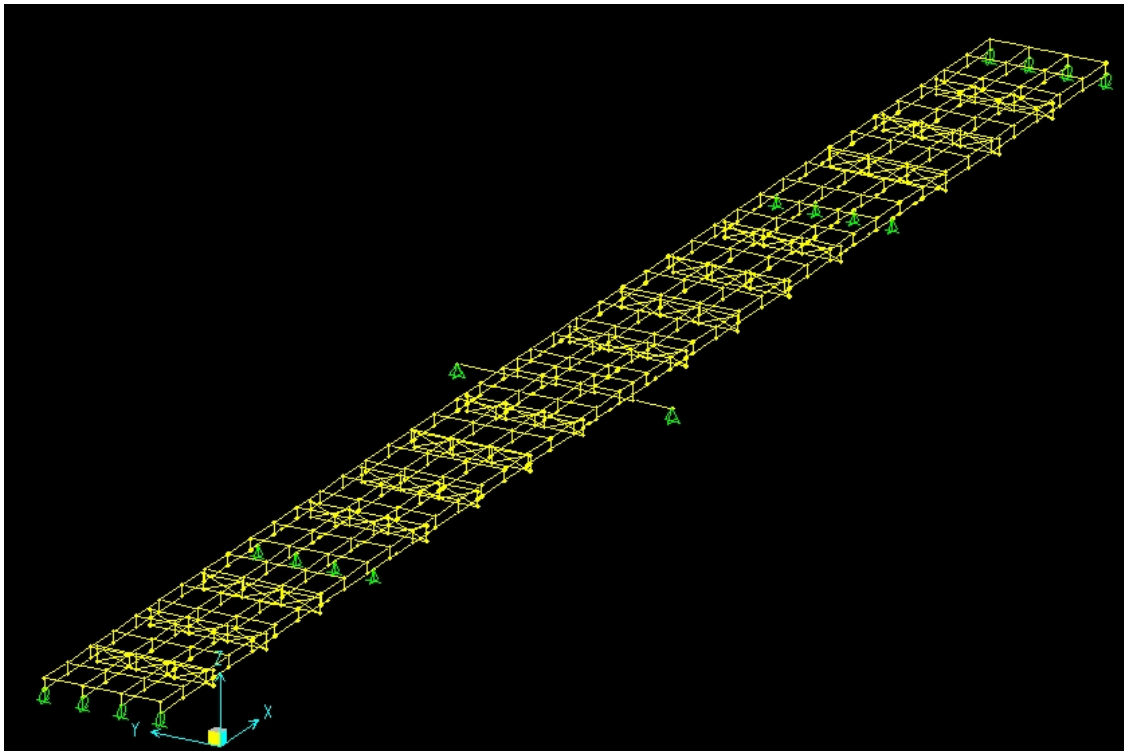


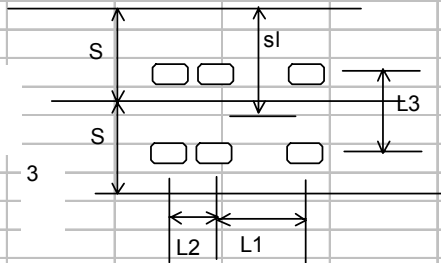
Figure 5.1: Three-dimensional grillage model

Several assumptions were made in the creation of the model. The strain gage readings indicated the concrete deck acted as a composite with the girders (Section 4.1.1). Therefore in the model the deck was attached with rigid links to the girders to simulate full composite action. At Piers 4, 5 and 6, the girder supports were assumed pinned, while at the expansion joints located at the ends of the continuous section rollers were used.

In the static load cases, loads were applied representing a 50-kip Mn/DOT truck located at midspan. Load cases were applied for the truck being in both the left and the right lane. To determine the amount of load to apply to each frame element the following table was used (Table 5.1). Each wheel was assumed to be a point load that would be distributed between the two girders that it lies between. Therefore the load would be applied among the three girders that are affected. Moments would also be created since the wheels are not located directly over the girder. These point loads and moments were then applied to the frame elements representing the concrete deck of the grillage model. In the static load case the second axle was positioned at midspan between Piers 4 and 5.

Table 5.1: Applied load calculations for 50-kip truck

Point Load and Moment Calculations For Bridge 69832 to Use in SAP				
Girder Spacing				
S =	112 inches			1
Distance from girder A to center of traffic lane.				
sl =	128 inches			2
Axle Spacings				
L1 =	176 inches			
L2 =	52 inches			
L3 =	78 inches			
Loads Distribution over Girders (kips)				
Girder	Overall	3rd Axle	2nd Axle	1st Axle
	Reaction	17.5	18.2	14.15
1	0.103	1.797	1.869	1.453
2a	0.397	6.953	7.231	5.622
2b	0.254	4.453	4.631	3.601
3	0.246	4.297	4.469	3.474
Moments about x-axis from these loads (k-in)				
		3rd Axle	2nd Axle	1st Axle
1		159.92	166.32	129.31
2		85.00	88.40	68.73
3		-244.92	-254.72	-198.04



The moving load cases followed the distribution of the load similar to that for the static load. In the moving load case, the load is moved along the entire length of the bridge in a specific lane. Four lanes were created to represent a vehicle in order to distribute the loads more accurately over the girders. These lanes were given eccentricities to match the location of the wheels. The appropriate loads were applied to each lane and they were applied simultaneously to represent the whole vehicle traveling over the bridge. Moving load cases were applied representing single 50-kip trucks in the right lane and left lanes, and 2 50-kip trucks in the right and left lanes similar to truck test 2.

The results from the static load cases and the moving load cases were then compared to the strain gage measurements taken during the truck tests and during live traffic (Figure 5.2 & Figure 5.3). Several variations of the grillage model were created to try and represent the bridge as closely as possible.

The initial model used a concrete deck of 6.75” thickness, which is what is stated in the construction drawings. This gave results that overestimated the stresses in the girders. Models were then constructed using a deck thickness of 9”. This is a reasonable assumption, since with resurfacing of the roadway over the years the thickness would increase. This model provided lower stresses than those from the 6.75” model.

The significance of the diaphragm was also investigated. In one model with a 9” deck thickness, the diaphragm elements were left out. In this model, a higher load concentration was found on the girder that the vehicle straddled. The models with the diaphragm implemented showed the load distributed more evenly over the girders, which more closely resembled the measured strains.

Lastly the impact of the railings was investigated. On the model that included the railings as an integral part of the bridge, the stresses were reduced as the bridge was further stiffened. This model, which had a 9” deck thickness and included diaphragms, produced stresses that most accurately modeled those measured.

Maximum Stresses MNDOT Truck in Right Lane

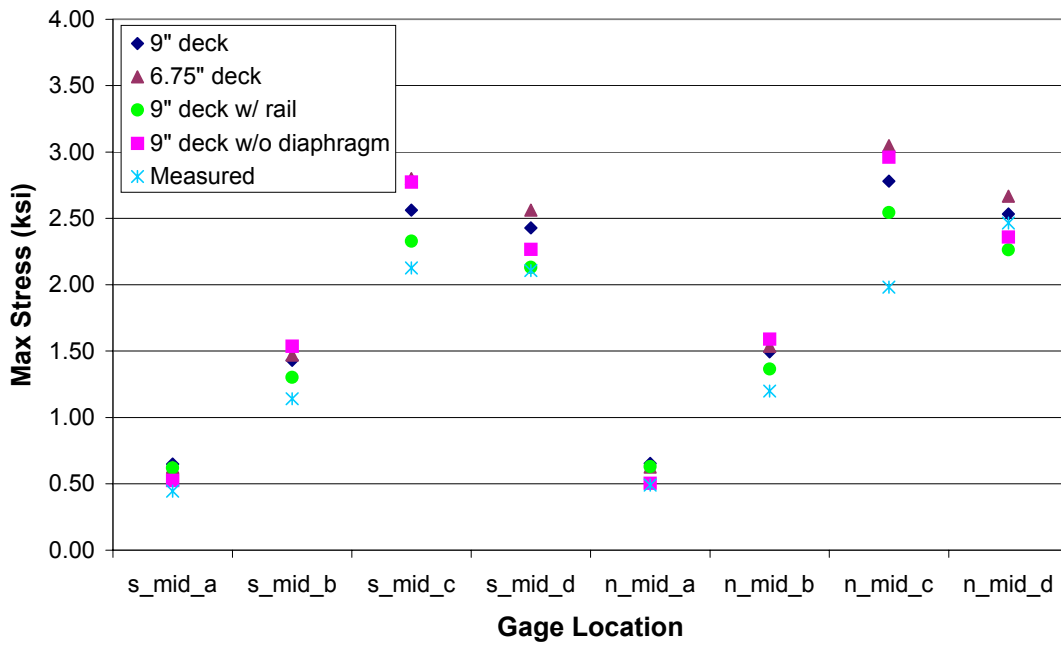


Figure 5.2: Stress comparison on bottom flange of girders at midspan for loading in the right lane

Maximum Stresses MNDOT Truck in Left Lane

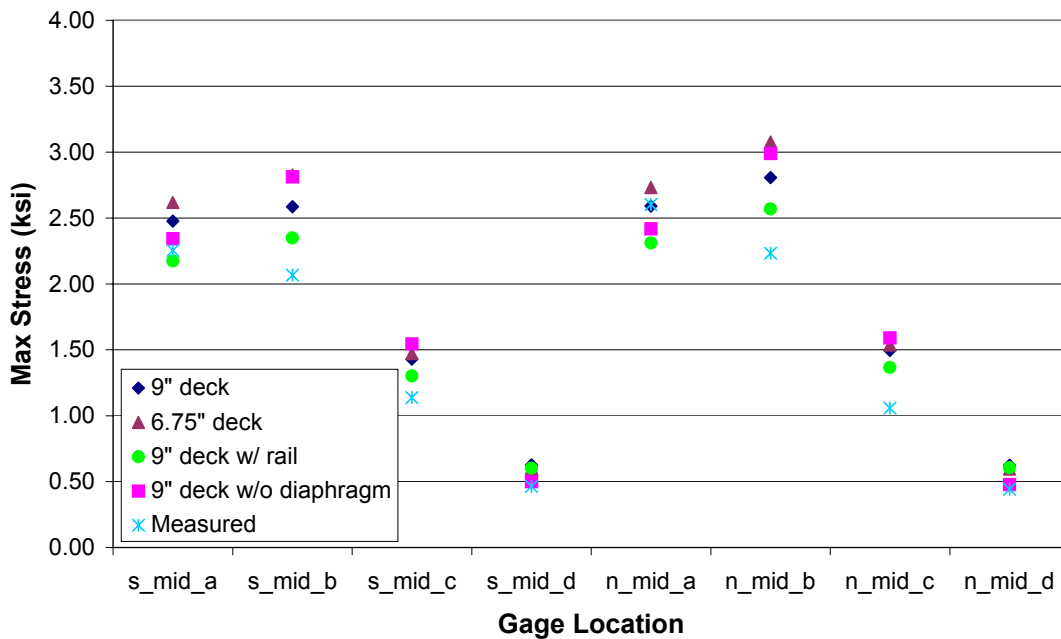


Figure 5.3: Stress comparison on bottom flange of girders at midspan for loading in the left lane

A comparison was also made of the stresses through the depth of the girder. Strain gages were placed at three locations through the depth at midspan. Figure 5.4 shows how the grillage models compare to the measurements taken for a 50-kip truck traveling in the right lane.

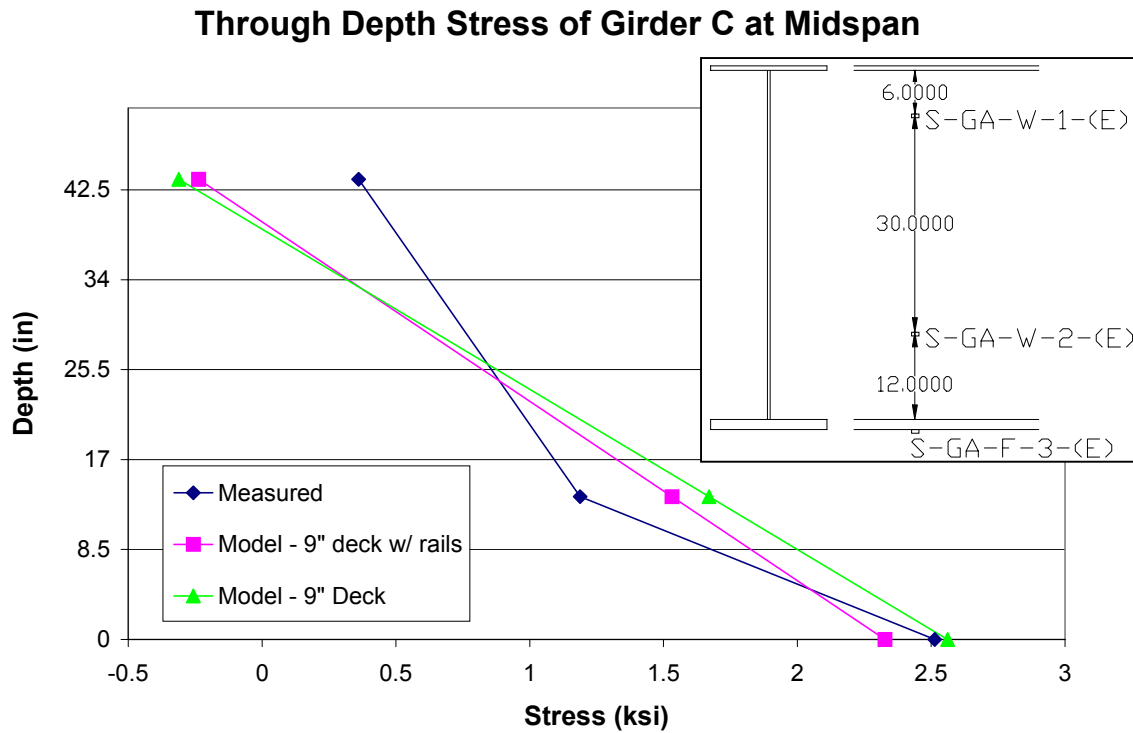


Figure 5.4: Through depth stresses on Girder C at midspan due to 50-kip truck

Using the influence lines from the moving load case of a single truck traveling in the right lane, the stress history as a vehicle travels across the bridge was created (Figure 5.5). The figure shows a comparison of the stress located at the bottom flange of girder C at midspan from the grillage model with a 9" deck and rails to that from the truck tests for a single 50-kip truck traveling in the right lane.

Midspan Girder C (MNDOT Truck in Right Lane)

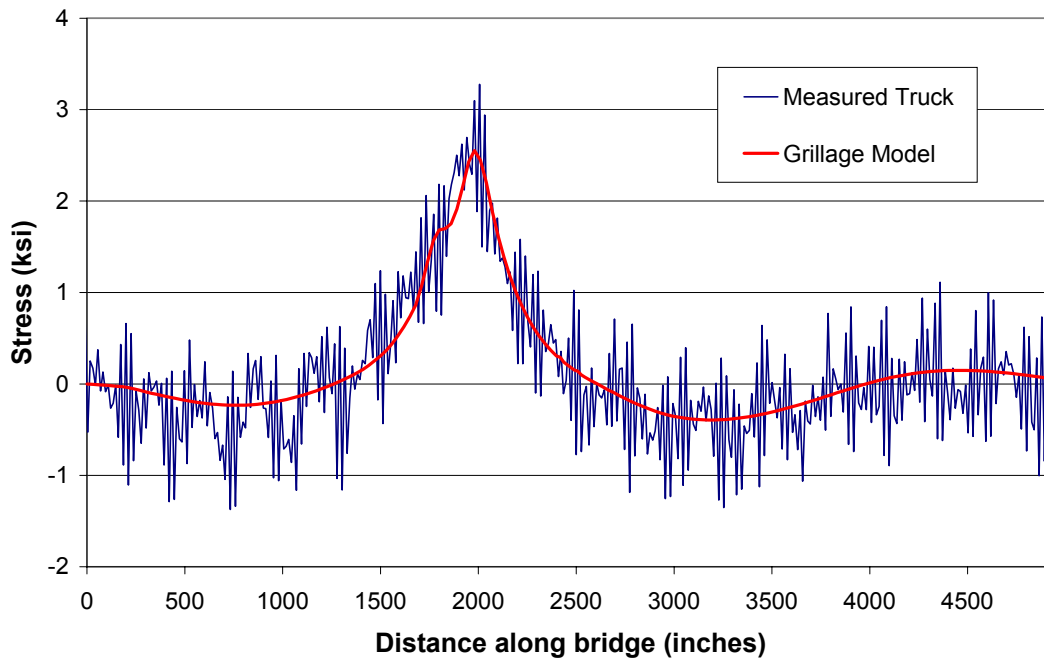


Figure 5.5: Stress history as load moves across the bridge

The 3-D grillage model provided a means to compare both moving and static loads to those recorded from the various instruments located on the bridge. The models all tended to overestimate the actual stresses, but as more details were included the results became more accurate. Usually the effect of rails and diaphragms are not included in the design of a bridge, but as shown they do have an effect on the load distribution as they aid in stiffening the structure.

5.2 Shell Element Models

The 3-D grillage model produced fairly accurate results for the overall performance of the bridge. To be able to understand the effects of loading on the areas experiencing fatigue problems the frame element did not provide enough information.

To be able to view the stresses and reaction of the stiffeners within the pier cap that are experiencing problems a shell element model was created that closely represented the details of the pier cap. This model depicted the steel box of the pier cap and included all the stiffeners located within the pier cap. It also modeled a section of the girders as they intersected the pier cap. This shell element model was then inserted into the grillage model replacing the frame elements that made up the pier cap and the portions of the girder modeled (Figure 5.6).

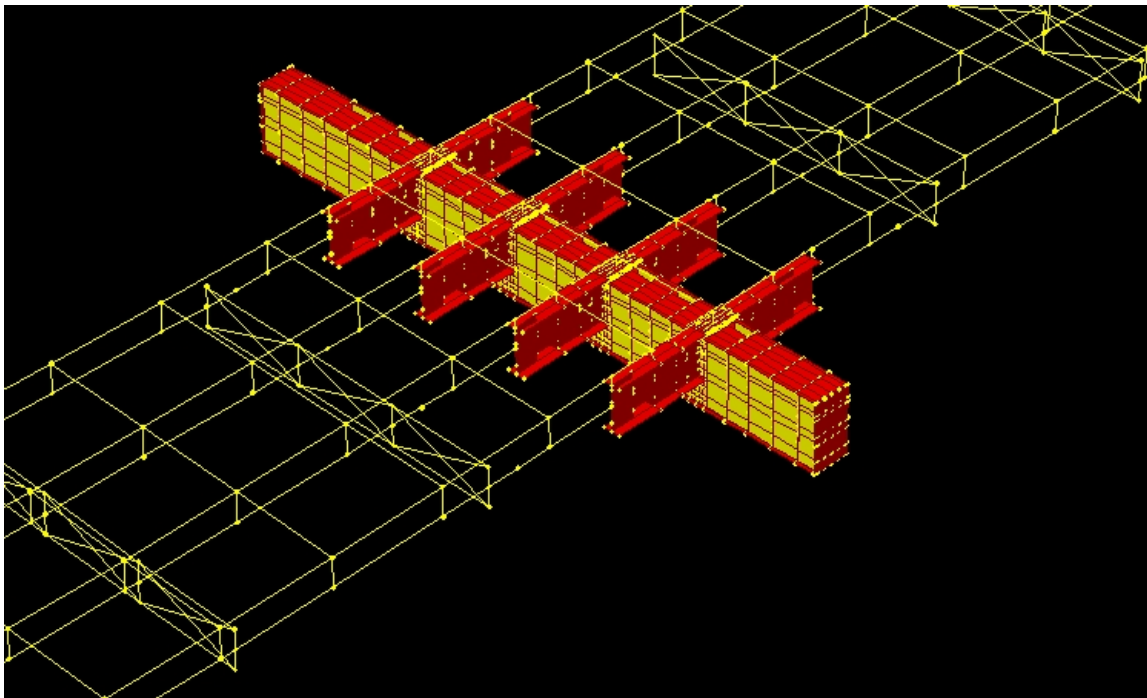


Figure 5.6: Shell element model integrated into grillage model

Assumptions made in representing the pier cap included making the supports at the piers pinned. Also all stiffeners were unattached to the bottom flange of the pier cap to model them as milled to bear following the construction plans.

Three different shell element models were created representing pier cap 5. One represented the pier cap assuming no cracks are present. The second assumes the cracks have propagated the full length of the stiffener. Lastly a model representing a retrofit option for the pier cap was modeled. A static load was applied to all three models at midspan representing a 50-kip Mn/DOT truck in the right lane.

5.2.1 Uncracked Model

In the uncracked model it was assumed the top of the stiffeners at the girder intersection were fully attached to the bottom flange of the girder. The strains measured from the strain gage for a theoretical 50-kip truck were converted to stresses and then compared to those at the approximate location on the shell element model to verify the replication of the pier cap.

5.2.2 Cracked Model

The cracked model assumed all the stiffeners at the girder intersections on the pier cap had cracked the full length. All of these stiffeners were released from the bottom flange of the girders, so they were very similar to the milled to bear surface at the bottom of the stiffener. This model was created to show how the stresses would be distributed if the pier cap was left alone and the cracks were allowed to propagate the full length.

5.2.3 Retrofit Model

The last model created represented the extreme case for a retrofit option. The stiffeners were left uncracked, while rigid links were attached connecting the bottom flange of the pier cap to the bottom flanges of the girders on the exterior of the pier cap. This fully stiffens the lower cell of the pier cap so the full box is forced to rotate with the girders. It alleviates the “soft story action” as the lower cell is restrained from shearing.

5.2.4 Comparison and Analysis

For comparison all three models were loaded with the equivalent of a 50-kip truck at midspan in the right lane.

To confirm the reliability of the model, the stresses from the stiffeners on the uncracked model were compared to the stresses obtained from the strains for a theoretical 50-kip truck in the right lane. Since only uncracked stiffeners were instrumented the uncracked model would most closely represent the measured results. Stresses at the locations of the strain gages on the stiffeners for the uncracked model, the cracked model, and the retrofitted model were obtained. Figure 5.7 shows these stresses compared to those that were determined from the field measurements.

Stiffener Stresses

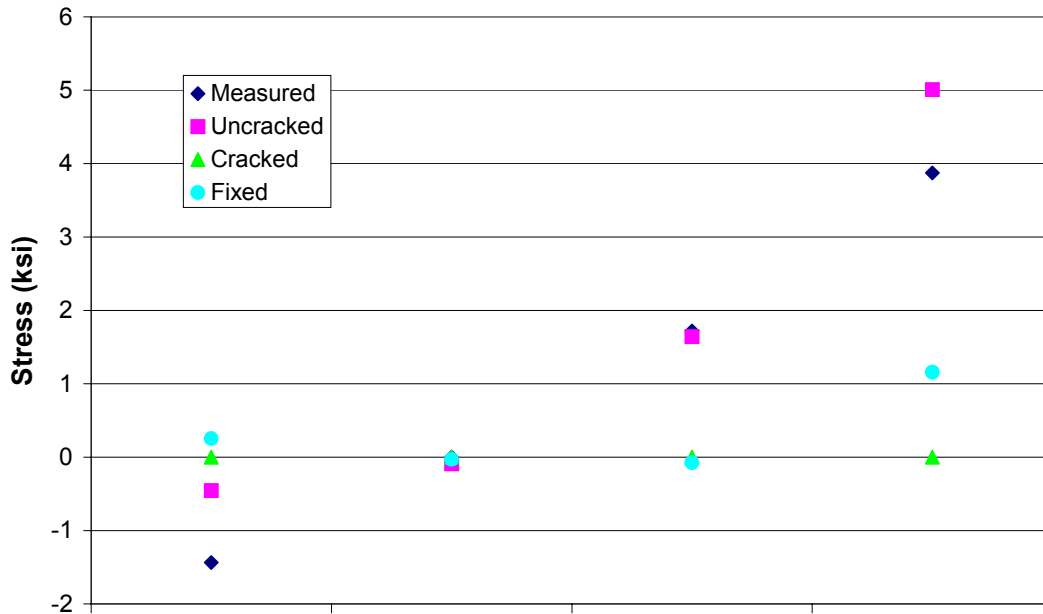


Figure 5.7: Stiffener stresses for the three shell element models

The uncracked model stresses were very similar to the measured stresses, especially in Girders B and C. In the cracked model all the stresses are relieved in the stiffeners hence the zero stress readings. The retrofitted or fixed model greatly reduces the stresses in the stiffeners as the full box of the pier cap is forced to rotate with the girder instead of the pier cap acting as two different stories. A stress distribution for the three different models at Girder D is shown in Figure 5.8. The first is the uncracked model as it shows the highest stress concentrations in the girder. The middle is the cracked model showing little to no stresses in the stiffeners. The last is the retrofitted model with the rigid links fixing the bottom cell.

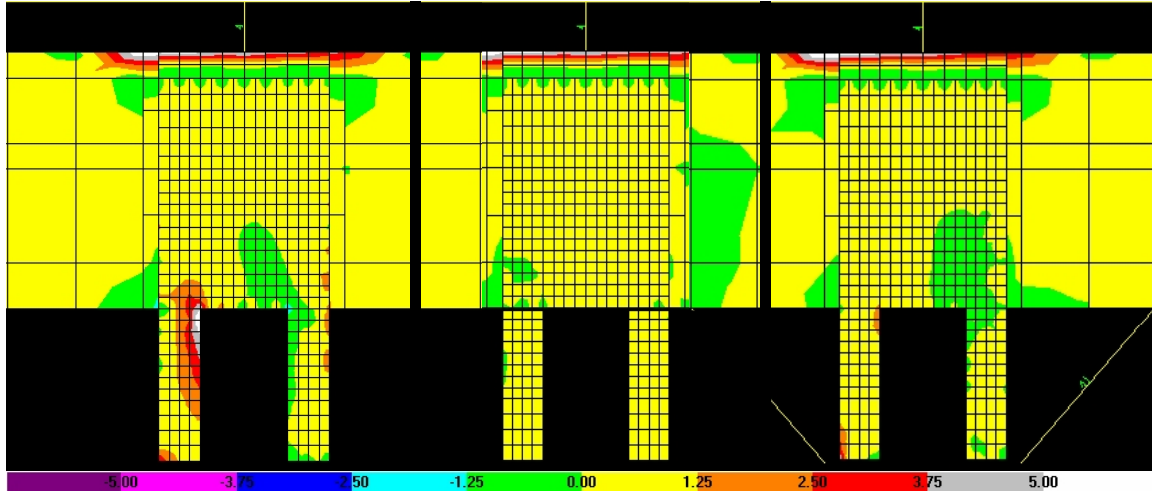


Figure 5.8: Stress distribution at Girder D for the three shell element models

In the cases of the uncracked model and the retrofitted model there was concern of where the stresses were redistributed in the pier cap to counter the torque being applied. The intermediate stiffeners located midway between the girders in the pier cap, were investigated to determine if they underwent any increase in stress.

The intermediate stiffeners are plates with an access hole cut in them, which run the full height of the pier cap (Figure 5.9). The edges are welded with two fillet welds on the top and the sides. The plate is milled to bear on the bottom.

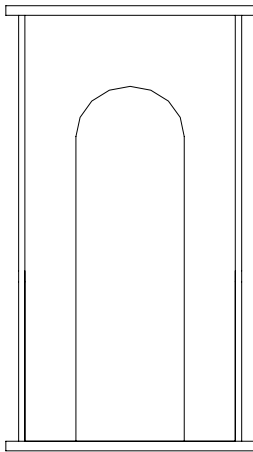


Figure 5.9: Intermediate stiffener detail

In the three shell element models the access hole was modeled as being rectangular instead of curved at the top due to the shape of the shell elements. Stresses were taken at the point just below the corners in the access opening. Figure 5.10 shows the results for the stresses in the intermediate stiffeners on the three models. This is also represented in the picture depicting the distribution of the stresses (Figure 5.11).

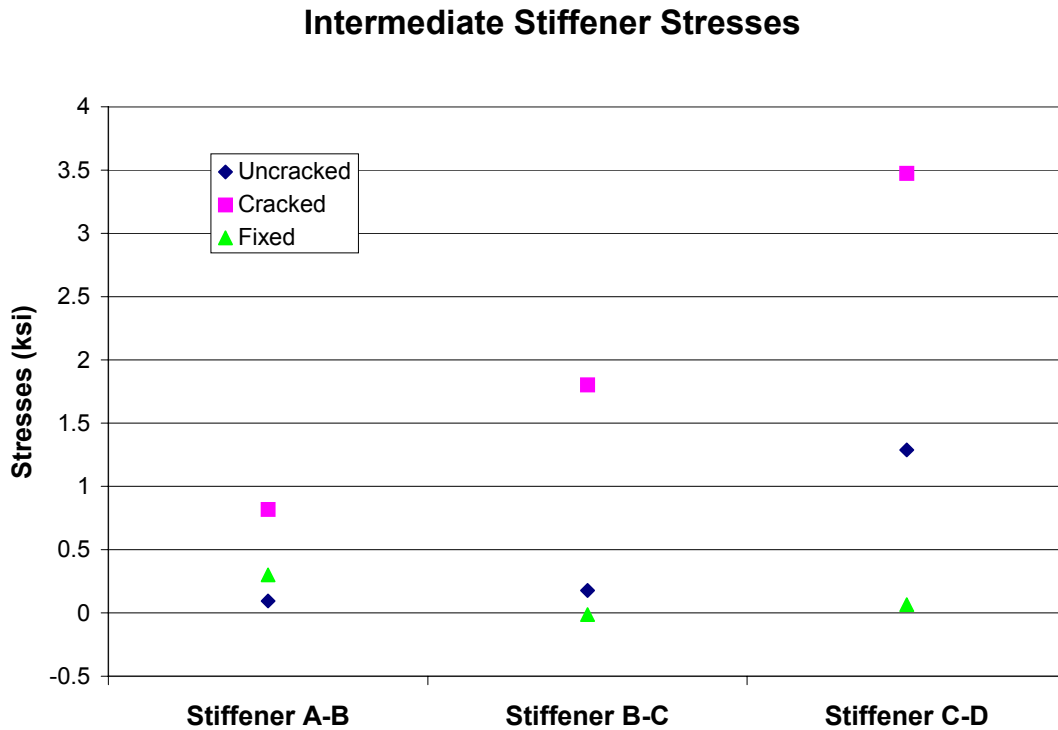


Figure 5.10: Maximum stresses in intermediate stiffeners due to 50-kip truck in right lane

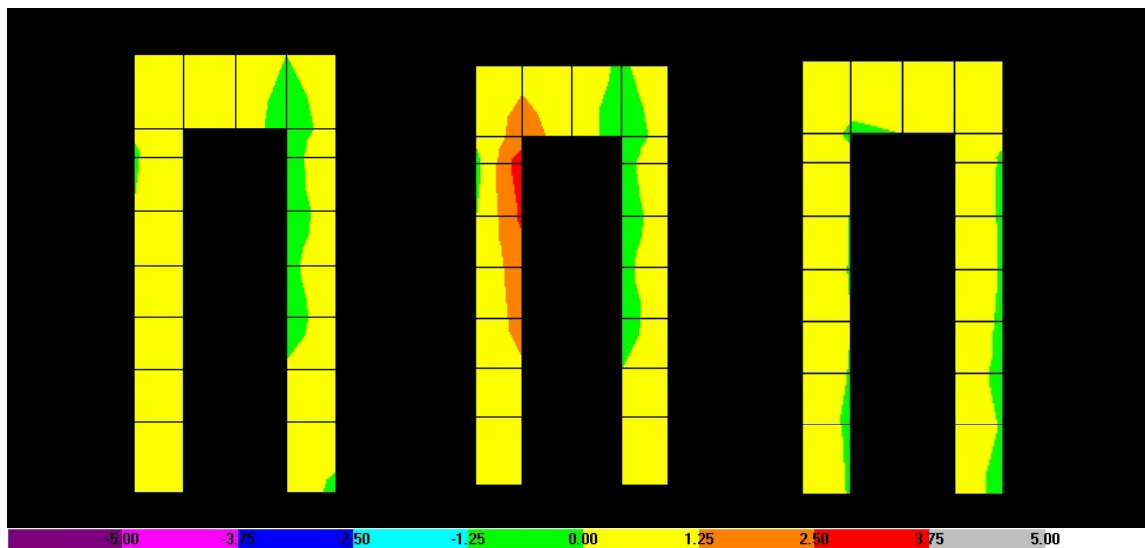


Figure 5.11: Stress distribution in intermediate Stiffener C-D

As shown in the uncracked model (the furthest on the left in the stress distribution), there is little resistance to the torsion of the pier cap carried in the intermediate stiffener. The stiffeners located at the girders provide the majority of the resistance.

In the cracked model since the stresses in the stiffeners at the girder intersection are relieved the section at this point is made more flexible. The burden of resisting torsion in the pier cap is transferred to the intermediate stiffeners. The stress is increased from approximately 0 ksi to 3.5 ksi in the intermediate stiffeners. This is still a relatively low stress range, and because of modeling the access opening as rectangular with a sharp point at the corner it may be somewhat magnified.

In the retrofitted or fixed model the stresses in the intermediate stiffeners are actually reduced slightly. The rigid links stiffen the girder intersection and reduce shearing deformation in the bottom cell. The deck, girders and the pier cap all move together as one unit, reducing any torsion in the pier cap.

CHAPTER 6: SUMMARY AND RECOMMENDATIONS

Bridge 69832 is a critical link in the flow of traffic heading into Duluth. Fatigue cracks have occurred in the fracture-critical steel pier caps with integral girders. A variety of sensors were installed at various locations near pier cap 5. Finite-element models were developed that agreed well with the measurements. It was confirmed that the cracks are due to torsion of the pier caps due to different girder end moments under traffic loading. As the rectangular cross section distorts, high stress ranges occur at the corners. The location of the high stress ranges is dependent on the detail inside the pier cap.

None of these cracks are presently a threat to the structural integrity of the pier caps. Most of the cracks are limited to the welds and will eventually arrest as they grow larger with minimal structural consequences. Therefore the recommendation for these cracks is to inspect them carefully every two years and not repair them. However, on the north side at Girder D of Pier Cap 9, the cracks are presently in the web plates of the pier caps and these must be repaired as soon as possible. Since there are three different crack types that have occurred, the recommendations for each are slightly different, as discussed below.

For further inspections of Bridge 69832 and bridges with similar integral pier caps, close attention should be paid to details that have stiffeners that are milled to bear at the tension flange instead of being attached. These details are susceptible to out of plane distortion. Also details that divide the pier cap into two cells where one cell is more flexible than the other. Larger deformation will concentrate in these more flexible cells and fatigue problems can occur at the corners. In older bridges especially, there is often poor welding. Poor fit up of the pieces may lead to gaps and associated inadequate weld throat. Welds with multiple passes, excess slag, gas pockets, and any other defects should be noted.

Similar pier caps with integral girders should be examined to estimate the distribution of the moments among the girders. If there is a large difference between the end moments of adjacent girders, there is a potential for these types of cracks. The next step would be to look at the detail and determine where the stress due to the torsion will concentrate.

6.1 Crack Type 1

Crack type 1 is the crack that is occurring at the weld connecting the top of the stiffener to the bottom of the girder flange continuity plate. Cracks like this have occurred at Girders A, B, and C on Pier Cap 5. All of these cracks are located on the stiffeners on the North side only.

Two different repair options are proposed for this crack type. The first option is to stiffen the intersection between the girder and pier cap. This would be achieved by bolting an angle to the bottom flange of the girder and the web of the pier cap (Figure 6.1). This would reduce the amount of shearing taking place in the lower cell of the pier cap, thus reducing the stress as shown in the retrofitted finite-element model.

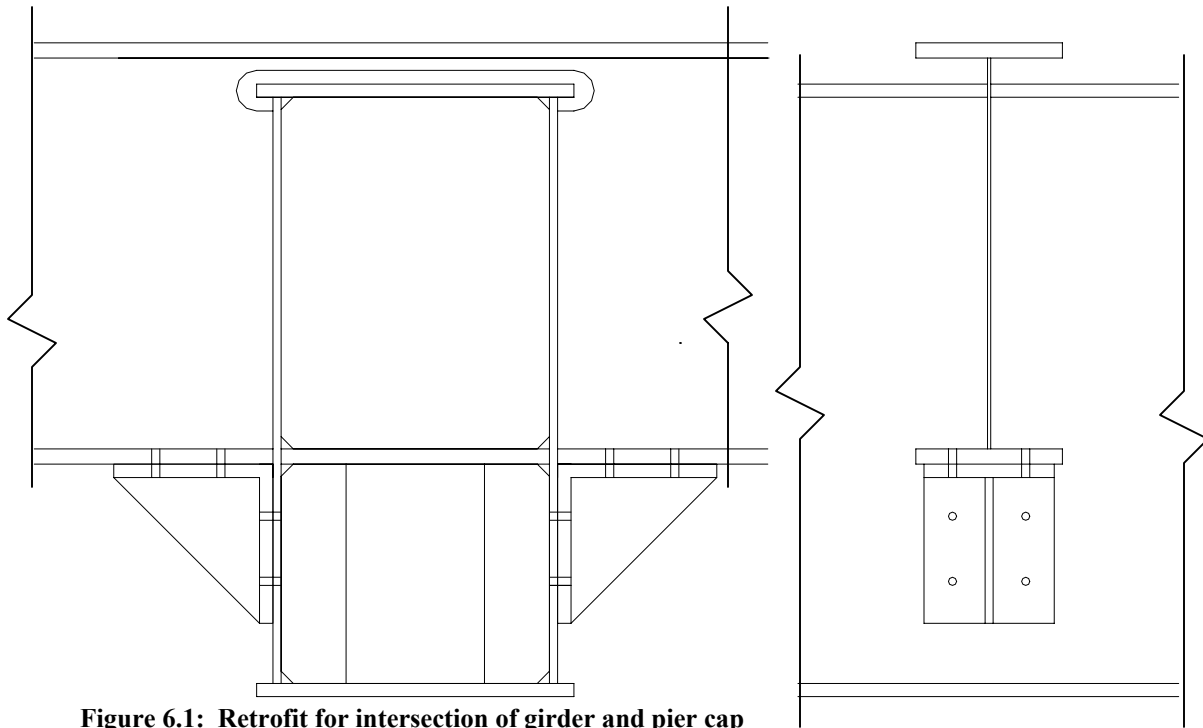


Figure 6.1: Retrofit for intersection of girder and pier cap

This option would not produce results as effective as that shown in the finite-element model. These are not rigid elements as modeled, and would still be subjected to some deformation. Also the expense to drill all the holes and install these stiffeners, which would have to be placed on both sides of the pier cap at each girder intersection, make it not the optimal solution.

The second option for crack type 1 is to let the cracks continue to grow until the stresses in the stiffeners are fully relieved. This eliminates the stress concentration on the stiffeners and makes the pier cap more flexible. As shown in the cracked finite element model, this places more stress on the intermediate stiffeners. This stress was found to be around 3.5 ksi for a 50 kip truck. This is well below the CAFL of 10 ksi for the intermediate stiffener, which is a category C detail. That stress is also more than likely inflated since the hole in the intermediate stiffener was modeled as rectangular instead of curved as it actually is. This option is far less expensive than the first and would only require the usual monitoring of the pier cap at both stiffener locations.

In the design of future pier caps, the stress ranges in these stiffeners must be estimated, considering the maximum difference between girder end moments. The size of the stiffener must be increased until the estimated stress range is less than the fatigue resistance, considering the reduction for cruciform connections in tension.

6.2 Crack Type 2

Crack type 2 occurs along the vertical welds connecting the bulkhead or full plate stiffener in the lower cell to the pier cap web. This crack type is caused by out-of-plane distortion of the web gap (8). Crack type 2 has occurred at girder D of pier cap 9 and Girders A and D of Pier Cap 11. The cracks on the north side in Girder D of Pier Cap 9 have propagated into the web of the pier cap, which is potentially a very serious condition. The other cracks have just propagated up the weld.

Since the pier cap is a fracture critical member, the cracks that have grown into the web on the north side in Girder D of Pier Cap 9 must be repaired. It has been shown that drilling four-inch diameter holes at the crack tips can arrest distortion-induced cracks (10). Cracks have reinitiated from smaller holes. Therefore, it is recommended that four-inch diameter holes be drilled in the pier cap web at the crack tips as shown in Figure 6.2, as soon as possible. These holes then should be covered and sealed to prevent debris, pigeons, and moisture from entering the interior of the pier cap.

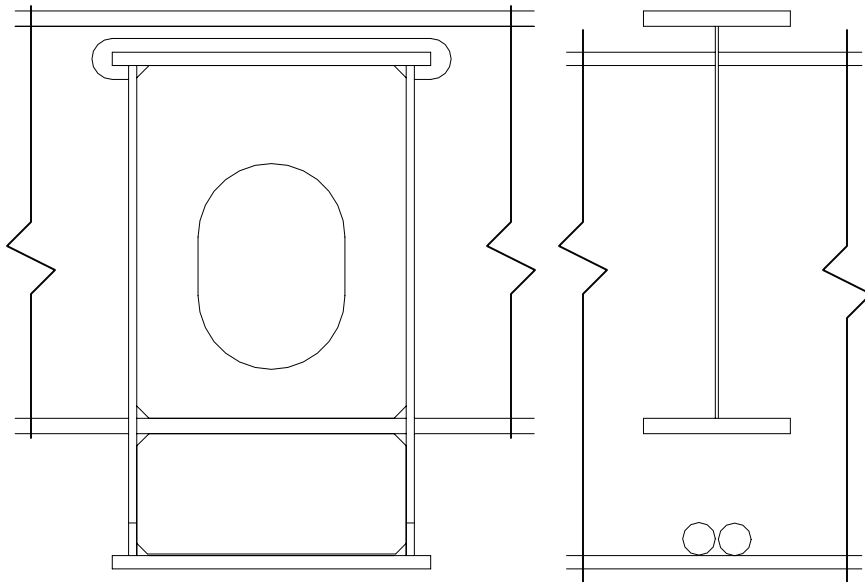


Figure 6.2: Hole drilling retrofit

For the type 2 cracks that have only propagated up the weld it is recommended that these continue to be monitored, but no repair is necessary. The crack increases the flexibility of the web gap and thus reduces the stress ranges for a specific distortion angle. Therefore these cracks are growing into a lower stress region and will soon arrest.

In future pier caps, the bulkhead should be continuously welded to the bottom flange of the pier cap with 5/16-inch fillet welds on both sides. This positive attachment should eliminate the web gap distortion and hence the potential for cracking.

6.3 Crack Type 3

Crack type 3 is located on the exterior of the pier cap on the weld connecting the girder web to the pier cap web. Only one crack of this type has occurred, at Girder C of pier cap 11 on the north side, and it hasn't propagated since it was first discovered.

For this crack it is recommended that no repair take place. Since this is in the negative moment region the tensile stresses are on the top half of the girder and compressive stresses are at the bottom. For this crack to grow it would have to propagate towards the compressive region. Therefore it would eventually stop growing if it hasn't already. Also since there is a cope around the flange of the pier cap in the girder web, there is no direct path for the crack to grow into the tensile flange of the girder where the higher stress ranges are located.

In the design of future pier caps, the stress range in the girder web must be estimated, considering the negative girder end moments. The web thickness may have to be increased to keep this stress range less than the allowable stress range for Category C. The cope hole should be carefully detailed to avoid sharp corners, and thermally cut edges must be ground.

REFERENCES

1. Minnesota Department of Transportation , “*Bridge Inspection Report: Bridge No. 69832*”. (Oakdale, MN: Minnesota Department of Transportation, June 22, 1999).
2. P. Wilson, W. Nelson, and D. Rychlak, “*Fracture Critical Bridge Inspection Report for Bridge #69832 Interstate 35/535 Interchange in Duluth*.” (Oakdale, MN: Minnesota Department of Transportation, 2001).
3. R.J. Dexter and J.W. Fisher, “Fatigue and Fracture,” chap. 53 in *Bridge Engineering Handbook*, ed. W.F. Chen (New York: CRC Press LLC, 2000).
4. J.W. Fisher, “The Evolution of Fatigue Resistant Steel Bridges.” in *1997 Distinguished Lectureship*, (Transportation Research Board, 76th Annual Meeting, Washington, D.C. Jan. 12-16, 1997) Paper No. 971520: 1-22.
5. American Association of State Highway and Transportation Officials (AASHTO) *LRFD, Bridge Design Specification* (Washington D.C. 2001).
6. *Manual of Steel Construction: Load and Resistance Factor Design, 3rd Edition*. (American Institute of Steel Construction, Inc. Chicago, 2000).
7. R.J. Dexter and J.W. Fisher, “Fatigue and Fracture,” chap 24 in *Handbook of Structural Engineering*, ed. W.F. Chen (New York: CRC Press LLC, 1997). pp 24-1 to 24-30.
8. J.W. Fisher, J. Jin, D.C. Wagner, and B.T. Yen, “*Distortion-Induced Fatigue Cracking in Steel Bridges*”. (Washington D.C.: Transportation Research Board, National Research Council, December 1990).
9. J.W. Fisher, B.M. Barthelemy, D.R. Mertz, and J.A. Edinger, “*Fatigue Behavior of Full-Scale Welded Attachments*,” (Washington D.C.: Transportation Research Board, National Research Council, November 1980).
10. J.C. McGormley, M.J. Koob, “*Large Hole Retrofits to Address Distortion-Induced Cracking*.” (Chicago: Wiss, Janey, Elstner Associates, Inc).
11. J.W. Fisher, “*Inspecting Steel Bridges for Fatigue Damage*.” (Bethlehem, PA: Lehigh University, 1981). Report No. 386-15(81).
12. H.M. O’Connell, and R.J. Dexter, “*Fatigue Evaluation of the Deck Truss of Bridge 9340*.” (Saint Paul, MN: Minnesota Department of Transportation, 2000).